

Learning Hash Function through Codewords

Yinjie Huang, *Student Member, IEEE*, Michael Georgiopoulos, *Member, IEEE*,
and Georgios C. Anagnostopoulos, *Member, IEEE*

Abstract—In this paper, we propose a novel hash learning approach that has the following main distinguishing features, when compared to past frameworks. First, the codewords are utilized in the Hamming space as ancillary techniques to accomplish its hash learning task. These codewords, which are inferred from the data, attempt to capture grouping aspects of the data's hash codes. Furthermore, the proposed framework is capable of addressing supervised, unsupervised and, even, semi-supervised hash learning scenarios. Additionally, the framework adopts a regularization term over the codewords, which automatically chooses the codewords for the problem. To efficiently solve the problem, one Block Coordinate Descent algorithm is showcased in the paper. We also show that one step of the algorithms can be casted into several Support Vector Machine problems which enables our algorithms to utilize efficient software package. For the regularization term, a closed form solution of the proximal operator is provided in the paper. A series of comparative experiments focused on content-based image retrieval highlights its performance advantages.

Index Terms—Hash Function Learning, Codewords, Block Coordinate Descent, SVM, Subgradient, Proximal Methods.

1 INTRODUCTION

WITH the eruptive growth of Internet data including images, music, documents and videos, content-based image retrieval (CBIR) has drawn lots of attention over the past few years [1]. Given a query sample from a user, a typical CBIR system retrieves samples stored in a database that are most similar to the query sample. The similarity is evaluated in terms of a pre-specified distance metric and the retrieved samples are the nearest neighbors of the query sample w.r.t. this metric. However, in some practical settings, exhaustively comparing the query sample with every sample in the database may be computationally expensive. Furthermore, most CBIR frameworks may be obstructed by the sheer size of each sample; for instance, visual descriptors of an image or a video may contain thousands of features. Additionally, storage of these high-dimensional data also presents a challenge.

Substantial effort has been invested in designing hash functions transforming the original data into compact binary codes to reap the benefits of a potentially fast similarity search. For example, when compact binary codes in Hamming space used, approximate nearest neighbors (ANN) [2] search was shown to achieve sub-linear searching time. Storage of the binary code is, obviously, also much more efficient. Furthermore, hash functions are typically designed to preserve certain similarity qualities between the data in the Hamming space.

Existing popular hashing approaches can be divided into two categories: *data-independent* and *data-dependent*. While the former category designs the hash function based on a non data-driven approach, the latter category, by inferring

from data, can be further clustered into supervised, unsupervised and semi-supervised learning tasks.

In this paper, we propose a novel hash function learning approach¹, dubbed *Supervised Hash Learning (*SHL) (* stands for all three learning paradigms), which exhibits the following advantages: first, the method uses a set of Hamming space codewords, that are learned during training, to capture the intrinsic similarities between the data's hash codes, so that same-class data are grouped together. Unlabeled data also contribute to the adjustment of codewords leveraging from the inter-sample dissimilarities of their generated hash codes, as measured by the Hamming distance metric. Additionally, a regularization term is utilized in our framework to move the codewords which represent the same class closer to each other. When some codewords collapse to one single codeword, our framework achieves automatic selection of the codewords. Due to these codeword-specific characteristics, a major advantage offered by our framework is that it can engage supervised, unsupervised and, even, semi-supervised hash learning tasks using a single formulation. Obviously, the latter ability readily allows the framework to perform transductive hash learning. Note that our framework can be viewed as an Error-Correction Codes (ECOC) method. Readers can refer to [4] and [5] for more details of ECOC.

In Sec. 3, we provide *SHL's formulation, which is mainly motivated by an attempt to minimize the within-group Hamming distances in the code space between a group's codeword and the hash codes of data that either should be similar (because of similar labels), or are de-facto similar (due to particular state of the hash functions). With regards to the hash functions, *SHL adopts a kernel-based approach. A new regularization term over codewords is also introduced for *SHL in its formulation. The aforementioned motivation eventually leads to a minimization problem over

1. A preliminary version of the work presented here has appeared in [3].

• Y. Huang and M. Georgiopoulos are with the Department of Electrical Engineering & Computer Science, University of Central Florida, Orlando, FL, 32826.

E-mail: yhuang@eeecs.ucf.edu, michaelg@ucf.edu

• G. C. Anagnostopoulos is with the Department of Electrical & Computer Engineering, Florida Institute of Technology, Melbourne, FL 32901.

E-mail: georgio@fit.edu

the codewords as well as over the Reproducing Kernel Hilbert Space (RKHS) vectors defining the hash functions. A quite noteworthy aspect of the resulting formulation is that the minimizations over the latter parameters leads to a set of Support Vector Machine (SVM) problems, according to which each SVM generates a single bit of a sample's hash code. In lieu of choosing a fixed, arbitrary kernel function, we use a simple Multiple Kernel Learning (MKL) approach (e.g. see [6]) to infer a good kernel from the data.

Next, in Sec. 4, an efficient Majorization-Minimization (MM) algorithm is showcased that can be used to optimize *SHL's framework via the Block Coordinate Descent (BCD) approaches. To train *SHL, the first block optimization amounts to training a set of SVM, which can be efficiently accomplished by using, for example, LIBSVM [7]. The second block optimization step addresses the MKL parameters. The third block involves solving a problem with the non-smooth regularization over codewords, which is optimized by Proximal Subgradient Descent (PSD). The second and third blocks are computationally fast thanks to closed-form solutions. When confronted with a huge data set, kernel related problem has computational limitation. In this work, a version of our algorithm for big data, which is based on the software LIBSKYLARK [8], is also presented.

Finally, in Sec. 6 we demonstrate the capabilities of *SHL on a series of comparative experiments. The section emphasizes on supervised hash learning problems in the context of CBIR. Additionally, we also apply the semi-supervised version of our framework on the foreground/background interactive image segmentation problems. Remarkably, when compared to other hashing methods on supervised learning hash tasks, *SHL exhibits the best retrieval accuracy in all the datasets we considered. Some clues to the method's superior performance are provided in Sec. 5.

2 RELATED WORK

As mentioned in Sec. 1, hashing methods can be divided into two categories: *data-independent* and *data-dependent*. The former category designs the hashing approaches without the necessity to infer from the data. For instance, in [9], Locality Sensitive Hashing (LSH) randomly projects and thresholds data into the Hamming space to generate binary codes. Data samples, which are closely located (in terms of Euclidean distances in the data's native space), are likely to have similar binary codes. Additionally, the authors of [10] proposed a method for ANN search through using a learned Mahalanobis metric combined with LSH. [11] introduces an encoding scheme based on random projections, in which the expected Hamming distance between two binary codes of the vectors is related to the value of a shift-invariant kernel.

On the other hand, *data-dependent methods* can, in turn, be grouped into supervised, unsupervised and semi-supervised learning paradigms.

The majority of work in data-dependent hashing approaches has been studied so far following the supervised learning scenario. For example, Semantic Hashing [12] designs the hash function using a Restricted Boltzmann Machine (RBM). Binary Reconstructive Embedding (BRE), proposed in [13], tries to minimize a cost function measuring the difference between the original metric distances and

the reconstructed distances in the Hamming space. In [14], through learning the hash functions from pair-wise side information, Minimal Loss Hashing (MLH) formulated the hashing problems based on a bound inspired by the theory of structural Support Vector Machines [15]. [16] addresses the scenario, where a small portion of sample pairs are manually labeled as similar or dissimilar and proposes the Label-regularized Max-margin Partition algorithm. Moreover, Self-Taught Hashing [17] first identifies binary codes for given documents via unsupervised learning; next, classifiers are trained to predict codes for query documents. Additionally, in [18], Fisher Linear Discriminant Analysis (LDA) was employed to embed the original data to a lower dimensional space and hash codes are obtained subsequently via thresholding. Boosting-based Hashing is used in [19] and [20], in which a set of weak hash functions are learned according to the boosting framework. In [21], the hash functions are learned from triplets of side information; their method is designed to preserve the relative comparison relationship from the triplets and is optimized using column generation. Furthermore, Kernel Supervised Hashing (KSH) [22] introduces a kernel-based hashing method, which seems to exhibit remarkable experimental results. Their method utilizes the equivalence between optimizing the code inner products and the Hamming distance. [23] proposes boosted decision trees for achieving non-linearity in hashing, which is fast to train. Their method employs an efficient GraphCut based block search approach. In [24], a supervised hash learning method for image retrieval is designed, in which their method automatically learns a good image representation tailored as well as several hash functions. Latent factor hashing, proposed in [25], learns similarity preserving compact binary codes based on a latent factor model. Finally, [26] combines structural Support Vector Machines with hashing methods to directly optimize over multivariate performance measure such as Area Under Curve (AUC).

Several approaches have also been proposed for unsupervised hashing: With the assumption of a uniform data distribution, Spectral Hashing (SPH) [27] designs the hash functions by utilizing spectral graph analysis. In [28], a new regularization is introduced to control the mismatch between the Hamming codes and the low-dimensional data representation. This new regularizer helps the methods better cope with the data sampled from a nonlinear manifold. Anchor Graph Hashing (AGH) [29] uses a small-size anchor graph to approximate low-rank adjacency matrices that leads to computational savings. Moreover, [30] proposed a projection learning method for error correction. Also, in [31], the authors introduce Iterative Quantization, which tries to learn an orthogonal rotation matrix so that the quantization error of mapping the data to the vertices of the binary hypercube is minimized. [32]'s idea is to decompose the feature space into a subspace shared by the hash functions. Then they design an objective function combining spectral embedding loss, binary quantization loss and shared subspace contribution. Finally, [33] presents an unsupervised hashing model based on graph model. Their method tries to preserve the neighborhood structure of massive data in a discrete code space.

As for semi-supervised hashing, there are a few ap-

proaches proposed: Semi-Supervised Hashing (SSH) in [30] and [34] minimizes an empirical error using labeled data; in order to avoid over-fitting, the framework also includes an information theoretic regularizer that utilizes both labeled and unlabeled data. Another method, semi-supervised tag hashing [35], incorporates tag information into training hash function by exploring the correlation between tags and hash bits. In [36], the authors introduce a hashing method integrating multiple modalities. Besides, semi-supervised information is also incorporated in the framework and a sequential learning scenario is adopted.

Finally, Let us note here that Self-Taught Hashing (STH) [17] employs SVMs to generate hash codes. However, STH differs significantly from *SHL; its unsupervised and supervised learning stages are completely decoupled, while our framework uses a single cost function that simultaneously accommodates both of these learning paradigms. Unlike STH, SVMs arise naturally from the problem formulation in *SHL.

3 FORMULATION

3.1 *Supervised Hash Learning

In what follows, $[\cdot]$ denotes the Iverson bracket, *i.e.*, $[\text{predicate}] = 1$, if the predicate is true, and $[\text{predicate}] = 0$, if otherwise. Additionally, vectors and matrices are denoted in boldface. All vectors are considered column vectors and \cdot^T denotes transposition. Also, for any positive integer K , we define $\mathbb{N}_K \triangleq \{1, \dots, K\}$.

Central to hash function learning is the design of functions transforming data to a compact binary codes in a Hamming space to fulfill a given machine learning task. Consider the Hamming space $\mathbb{H}^B \triangleq \{-1, 1\}^B$, which implies B -bit hash codes. *SHL addresses multi-class classification tasks with an arbitrary set \mathcal{X} as sample space. It does so by learning a hash function $\mathbf{h} : \mathcal{X} \rightarrow \mathbb{H}^B$ and a set of $C \times S$ labeled codewords $\boldsymbol{\mu}_{c,s}$, $c \in \mathbb{N}_C$ and $s \in \mathbb{N}_S$ (Each class is represented by S codewords), so that the hash code of a labeled sample is mapped close to the codeword corresponding to the sample's class label, where proximity is measured via the Hamming distance. Unlabeled samples are also able to contribute in learning both the hash function and the codewords as it will be demonstrated in the sequel. Finally, a test sample is classified according to the label of the codeword closest to the sample's hash code.

In *SHL, the hash code for a sample $x \in \mathcal{X}$ is eventually computed as $\mathbf{h}(x) \triangleq \text{sgn} \mathbf{f}(x) \in \mathbb{H}^B$, where the signum function is applied component-wise. Furthermore, $\mathbf{f}(x) \triangleq [f_1(x) \dots f_B(x)]^T$, where $f_b(x) \triangleq \langle w_b, \phi(x) \rangle_{\mathcal{H}_b} + \beta_b$ with $w_b \in \Omega_{w_b} \triangleq \{w_b \in \mathcal{H}_b : \|w_b\|_{\mathcal{H}_b} \leq R_b, R_b > 0\}$ and $\beta_b \in \mathbb{R}$ for all $b \in \mathbb{N}_B$. In the previous definition, \mathcal{H}_b is a RKHS with inner product $\langle \cdot, \cdot \rangle_{\mathcal{H}_b}$, induced norm $\|w_b\|_{\mathcal{H}_b} \triangleq \sqrt{\langle w_b, w_b \rangle_{\mathcal{H}_b}}$ for all $w_b \in \mathcal{H}_b$, associated feature mapping $\phi_b : \mathcal{X} \rightarrow \mathcal{H}_b$ and reproducing kernel $k_b : \mathcal{X} \times \mathcal{X} \rightarrow \mathbb{R}$, such that $k_b(x, x') = \langle \phi_b(x), \phi_b(x') \rangle_{\mathcal{H}_b}$ for all $x, x' \in \mathcal{X}$. Instead of a priori selecting the the kernel functions k_b , MKL [6] is employed to infer the feature mapping for each bit from the available data. In specific, it is assumed that each RKHS \mathcal{H}_b is formed as the direct sum of M common, pre-specified RKHSs \mathcal{H}_m , *i.e.*, $\mathcal{H}_b = \bigoplus_m \sqrt{\theta_{b,m}} \mathcal{H}_m$, where $\theta_b \triangleq$

$[\theta_{b,1} \dots \theta_{b,M}]^T \in \Omega_\theta \triangleq \left\{ \boldsymbol{\theta} \in \mathbb{R}^M : \boldsymbol{\theta} \succeq \mathbf{0}, \|\boldsymbol{\theta}\|_p \leq 1, p \geq 1 \right\}$, \succeq denotes the component-wise \geq relation, $\|\cdot\|_p$ is the usual l_p norm in \mathbb{R}^M and m ranges over \mathbb{N}_M . Note that, if each preselected RKHS \mathcal{H}_m has associated kernel function k_m , then it holds that $k_b(x, x') = \sum_m \theta_{b,m} k_m(x, x')$ for all $x, x' \in \mathcal{X}$.

Now, assume a training set of size N consisting of labeled and unlabeled samples and let \mathcal{N}_L and \mathcal{N}_U be the index sets for these two subsets respectively. Let also l_n for $n \in \mathcal{N}_L$ be the class label of the n^{th} labeled sample. By adjusting its parameters, which are collectively denoted as $\boldsymbol{\omega}$, *SHL attempts to reduce the distortion measure

$$E(\boldsymbol{\omega}) \triangleq \sum_{n \in \mathcal{N}_L} \min_s d(\mathbf{h}(x_n), \boldsymbol{\mu}_{l_n, s}) + \sum_{n \in \mathcal{N}_U} \min_{c, s} d(\mathbf{h}(x_n), \boldsymbol{\mu}_{c, s}) \quad (1)$$

where d is the Hamming distance defined as $d(\mathbf{h}, \mathbf{h}') \triangleq \sum_b [h_b \neq h'_b]$. Note that for each sample, one best codeword of each class will be selected to represent it. However, the distortion E is difficult to directly minimize. As it will be illustrated further below, an upper bound \bar{E} of E will be optimized instead.

In particular, for a hash code produced by *SHL, it holds that $d(\mathbf{h}(x), \boldsymbol{\mu}) = \sum_b [\mu^b f_b(x) < 0]$. If one defines $\bar{d}(\mathbf{f}, \boldsymbol{\mu}) \triangleq \sum_b [1 - \mu^b f_b]_+$, where $[u]_+ \triangleq \max\{0, u\}$ is the hinge function, then $d(\text{sgn} \mathbf{f}, \boldsymbol{\mu}) \leq \bar{d}(\mathbf{f}, \boldsymbol{\mu})$ holds for every $\mathbf{f} \in \mathbb{R}^B$ and any $\boldsymbol{\mu} \in \mathbb{H}^B$. Based on this latter fact, it holds that

$$E(\boldsymbol{\omega}) \leq \bar{E}(\boldsymbol{\omega}) \triangleq \sum_c \sum_s \sum_n \gamma_{c,n,s} \bar{d}(\mathbf{f}(x_n), \boldsymbol{\mu}_{c,s}) \quad (2)$$

where

$$\gamma_{c,n,s} \triangleq \begin{cases} [c = l_n] [s = \arg \min_{s'} \bar{d}(\mathbf{f}(x_n), \boldsymbol{\mu}_{l_n, s'})] & n \in \mathcal{N}_L \\ [(c, s) = \arg \min_{c', s'} \bar{d}(\mathbf{f}(x_n), \boldsymbol{\mu}_{c', s'})] & n \in \mathcal{N}_U \end{cases} \quad (3)$$

It turns out that \bar{E} , which constitutes the model's loss function, can be efficiently minimized by a three-step algorithm, which delineated in the next section.

4 LEARNING ALGORITHM

4.1 Algorithm for *SHL

The next proposition allows us to minimize \bar{E} as defined in Eq. (2) via a MM approach [37] and [38].

Proposition 1. For any *SHL parameter values $\boldsymbol{\omega}$ and $\boldsymbol{\omega}'$, it holds that

$$\bar{E}(\boldsymbol{\omega}) \leq \bar{E}(\boldsymbol{\omega}|\boldsymbol{\omega}') \triangleq \sum_c \sum_s \sum_n \gamma'_{c,n,s} \bar{d}(\mathbf{f}(x_n), \boldsymbol{\mu}_{c,s}) \quad (4)$$

where the primed quantities are evaluated on $\boldsymbol{\omega}'$ and

$$\gamma'_{c,n,s} \triangleq \begin{cases} [c = l_n] [s = \arg \min_{s'} \bar{d}(\mathbf{f}'(x_n), \boldsymbol{\mu}'_{l_n, s'})] \\ n \in \mathcal{N}_L \\ [(c, s) = \arg \min_{c', s'} \bar{d}(\mathbf{f}'(x_n), \boldsymbol{\mu}'_{c', s'})] \\ n \in \mathcal{N}_U \end{cases} \quad (5)$$

Additionally, it holds that $\bar{E}(\boldsymbol{\omega}|\boldsymbol{\omega}) = \bar{E}(\boldsymbol{\omega})$ for any $\boldsymbol{\omega}$. In summa, $\bar{E}(\cdot|\cdot)$ majorizes $\bar{E}(\cdot)$.

Its proof is relative straightforward and is based on the fact that for any value of $\gamma'_{c,n,s} \in \{0, 1\}$ other than $\gamma_{c,n,s}$ as defined in Eq. (3), the value of $\bar{E}(\boldsymbol{\omega}|\boldsymbol{\omega}')$ can never be less than $\bar{E}(\boldsymbol{\omega}|\boldsymbol{\omega}) = \bar{E}(\boldsymbol{\omega})$.

The last proposition gives rise to a MM approach, where $\boldsymbol{\omega}'$ are the current estimates of the model's parameter values and $\bar{E}(\boldsymbol{\omega}|\boldsymbol{\omega}')$ is minimized with respect to $\boldsymbol{\omega}$ to yield improved estimates $\boldsymbol{\omega}^*$, such that $\bar{E}(\boldsymbol{\omega}^*) \leq \bar{E}(\boldsymbol{\omega}')$. This minimization can be achieved via a BCD, as is argued based on the next proposition.

Proposition 2. *Minimizing $\bar{E}(\cdot|\boldsymbol{\omega}')$ with respect to the Hilbert space vectors, the offsets β_p and the MKL weights $\boldsymbol{\theta}_b$, while regarding the codeword parameters as constant, one obtains the following B independent, equivalent problems:*

$$\begin{aligned} \inf_{\substack{w_{b,m} \in \mathcal{H}_m, m \in \mathbb{N}_M \\ \beta_b \in \mathbb{R}, \boldsymbol{\theta}_b \in \Omega_{\boldsymbol{\theta}}, \mu_{c,s}^b \in \mathbb{H}}} & \lambda_1 \sum_c \sum_s \sum_n \gamma'_{c,n,s} [1 - \mu_{c,s}^b f_b(x_n)]_+ \\ & + \frac{1}{2} \sum_m \frac{\|w_{b,m}\|_{\mathcal{H}_m}^2}{\theta_{b,m}} \\ & + \lambda_2 \sum_c \sum_{i,j \in S} \|\boldsymbol{\mu}_{c,i} - \boldsymbol{\mu}_{c,j}\|_2 \quad b \in \mathbb{N}_B \end{aligned} \quad (6)$$

where $f_b(x) = \sum_m \langle w_{b,m}, \phi_m(x) \rangle_{\mathcal{H}_m} + \beta_b$ and $\lambda_1 > 0$ is a regularization constant.

The proof of this proposition hinges on replacing the (independent) constraints of the Hilbert space vectors with equivalent regularization terms and, finally, performing the substitution $w_{b,m} \leftarrow \sqrt{\theta_{b,m}} w_{b,m}$ as typically done in such MKL formulations (e.g. see [6]). The third term in Prob. (6) pushes codewords representing the same class closer to each other. With an appropriate value of λ_2 , this regularization helps *SHL automatically select the codewords.

Note that Prob. (6) is jointly convex with respect to all variables under consideration and, under closer scrutiny, one may recognize it as a binary MKL SVM training problem, which will become more apparent shortly.

First block minimization: By considering $w_{b,m}$ and β_b for each b as a single block, instead of directly minimizing Prob. (6), one can instead maximize the following problem:

Proposition 3. *The dual form of Prob. (6) takes the form of*

$$\sup_{\boldsymbol{\alpha}_b \in \Omega_{\boldsymbol{\alpha}_b}} \boldsymbol{\alpha}_b^T \mathbf{1}_{NCs} - \frac{1}{2} \boldsymbol{\alpha}_b^T \mathbf{D}_b [(\mathbf{1}_{CS} \mathbf{1}_{CS}^T) \otimes \mathbf{K}_b] \mathbf{D}_b \boldsymbol{\alpha}_b \quad b \in \mathbb{N}_B \quad (7)$$

where $\mathbf{1}_K$ stands for the all ones vector of K elements ($K \in \mathbb{N}$), $\boldsymbol{\mu}_b \triangleq [\mu_{1,b} \dots \mu_{C,b}]^T$, $\mathbf{D}_b \triangleq \text{diag}(\boldsymbol{\mu}_b \otimes \mathbf{1}_N)$, $\mathbf{K}_b \triangleq \sum_m \theta_{b,m} \mathbf{K}_m$, where \mathbf{K}_m is the data's m^{th} kernel matrix, $\Omega_{\boldsymbol{\alpha}_b} \triangleq$

$$\{\boldsymbol{\alpha} \in \mathbb{R}^{NC} : \boldsymbol{\alpha}_b^T (\boldsymbol{\mu}_b \otimes \mathbf{1}_N) = 0, \mathbf{0} \preceq \boldsymbol{\alpha}_b \preceq \lambda_1 \boldsymbol{\gamma}'\} \text{ and } \boldsymbol{\gamma}' \triangleq [\gamma'_{1,1,1}, \dots, \gamma'_{1,N,1}, \gamma'_{1,N,2}, \dots, \gamma'_{1,N,S}, \gamma'_{2,N,S}, \dots, \gamma'_{C,N,S}]^T.$$

The detailed proof is provided in Appendix A. Given that $\gamma'_{c,n,s} \in \{0, 1\}$, one can easily now recognize that Prob. (7) is a SVM training problem, which can be conveniently solved using software packages such as LIBSVM. After solving it, obviously one can compute the quantities $\langle w_{b,m}, \phi_m(x) \rangle_{\mathcal{H}_m}$, β_b and $\|w_{b,m}\|_{\mathcal{H}_m}^2$, which are required in the next step.

When dealing with large scale data sets, the sequential solver LIBSVM may encounter the memory bottleneck because of the kernel matrix computation. Therefore a parallel software package is necessary for big data problems. LIBSKYLARK [8], which utilizes random features [39] to approximate kernel matrix and Alternating Direction Method of Multipliers (ADMM) [40] to parallelize the algorithm, proves to be an efficient solver for large scale SVM problem. LIBSKYLARK achieves impressive acceleration when solving SVM compared to LIBSVM in [8]. Experiments over large data sets are also conducted in Sec. 6.

Second block minimization: Having optimized the SVM parameters, one can now optimize the cost function of Prob. (6) with respect to the MKL parameters $\boldsymbol{\theta}_b$ as a single block using the closed-form solution mentioned in Prop. 2 of [6] for $p > 1$, which is given below

$$\theta_{b,m} = \frac{\|w_{b,m}\|_{\mathcal{H}_m}^{\frac{2}{p+1}}}{\left(\sum_{m'} \|w_{b,m'}\|_{\mathcal{H}_{m'}}^{\frac{2p}{p+1}}\right)^{\frac{1}{p}}}, \quad m \in \mathbb{N}_M, b \in \mathbb{N}_B. \quad (8)$$

Third block minimization: we need to optimize this problem due to the new regularization introduced:

$$\begin{aligned} \inf_{\mu_{c,s}^b \in \mathbb{H}} & \sum_n \sum_c \sum_s \gamma'_{c,n,s} [1 - \mu_{c,s}^b f_b(x_n)]_+ \\ & + \lambda_2 \sum_c \sum_{i,j \in S} \|\boldsymbol{\mu}_{c,i} - \boldsymbol{\mu}_{c,j}\|_2 \end{aligned} \quad (9)$$

Here, $c \in \mathbb{N}_C$, $b \in \mathbb{N}_B$, $s \in \mathbb{N}_S$.

First of all, we relax $\boldsymbol{\mu}$ to continuous values, similar to relaxing the hashcode as continuous when computing the hinge loss. Eq. (9) follows the formulation $l(\mathbf{x}) + h(\mathbf{x})$, which can be solved by proximal methods [41]. Since both the terms (hinge loss and regularization) are convex and non-smooth, we employ PSD method in a similar fashion as in [42], [43] and [44].

The proximal subgradient descent is

$$\mathbf{x}^{k+1} := \text{prox}_{\eta h}(\mathbf{x}^k - \eta \partial l(\mathbf{x}^k)) \quad (10)$$

where η is the step length and ∂l is the subgradient of the function. Here the proximal operator **prox** is defined as:

$$\text{prox}_{\eta h}(\mathbf{v}) \triangleq \arg \min_{\mathbf{x}} \left(h(\mathbf{x}) + \frac{1}{2\eta} \|\mathbf{x} - \mathbf{v}\|_2^2 \right) \quad (11)$$

To obtain proximal operator, one needs to solve Eq. (11). In our problem setting, the regularization is the sum of many non smooth L_2 norms, whose closed form proximal

operator is not obvious to achieve. Based on the conclusion from [45], the proximal operator of sums of the functions can be approximated by sums of the proximal operator of the individual function, i.e. $\text{prox}_{\sum h} \approx \sum \text{prox}_h$. Thus, all we need is the closed form proximal operator for one individual norm in Eq. (9), i.e. $\sum_{i,j \in S} \|\mu_i - \mu_j\|_2$. Let us concatenate all codewords as $\mu = [\mu_1^T, \dots, \mu_S^T]^T \in \mathbb{R}^{BS}$. Moreover, a vector is defined as $\mathbf{o} \triangleq [0, \dots, 1, \dots, -1, \dots, 0] \in \mathbb{R}^S$, where the value for index i is set to 1 and -1 for index j . With the definition of a matrix $U \triangleq \mathbf{o} \otimes I_B \in \mathbb{R}^{B \times BS}$, the regularization can be reformulated as $h(\mu) = \|U\mu\|_2$, whose proximal operator will be given in the following proposition:

Proposition 4. *Given the norm as: $h(\mu) = \|U\mu\|_2$. Following the definition in Eq. (11), the proximal operator of this norm:*

$$\text{prox}_{\eta h}(v) = \begin{cases} \mu_1 = v_1 \\ \vdots \\ \mu_i = \alpha_1 v_i + \alpha_2 v_j \\ \vdots \\ \mu_j = \alpha_2 v_i + \alpha_1 v_j \\ \vdots \\ \mu_S = v_S \end{cases} \quad (12)$$

where $\alpha_1 = 1 - \alpha_2$ and $\alpha_2 = \min\{\frac{\eta}{\|v_i - v_j\|_2}, \frac{1}{2}\}$, $v = [v_1^T, \dots, v_S^T]^T$, which is the input vector for proximal operators in Eq. (11).

The detailed proof of Prop. 4 is showcased in Appendix B.

Note that, if we consider only one codeword for each class, Prob. (9) can be simplified without the regularization:

$$\inf_{\mu_c^b \in \mathbb{H}} \sum_n \sum_c \gamma'_{c,n} \left[1 - \mu_c^b f_b(x_n) \right]_+ \quad (13)$$

Prob. (13) can be optimized by mere substitution.

On balance, as summarized in Algorithm 1, for each bit, the algorithm to *SHL consists of one SVM optimization and one MKL update. For the third step, we evaluate the proximal operator for each regularization and compute the summation to do the PSD to optimize codewords. Note that accelerated proximal gradient descent [46] is utilized here. $\gamma'_{c,n,s}$ is then updated according to the current estimate of the parameters. This algorithm, as shown in Algorithm 1, continues running until reaching the convergence². Based on LIBSVM, which provides $\mathcal{O}(N^3)$ complexity [47], our algorithm offers the complexity $\mathcal{O}(BN^3)$ per iteration, where B is the code length and N is the number of instances.

5 INSIGHTS TO GENERALIZATION PERFORMANCE

The superior performance of *SHL over other state-of-the-art hash function learning approaches featured in the next section can be explained to some extent by noticing that

² MATLAB[®] code of *SHL's algorithm will be made publicly accessible, upon this manuscript's acceptance by the journal.

Algorithm 1 Optimization of Prob. (6)

Input: Bit Length B , Training Samples X containing labeled or unlabeled data.

Output: ω .

1. Initialize ω .
2. **While Not Converged**
3. **For each bit**
4. $\gamma'_{g,n,s} \leftarrow \text{Eq. (5)}$.
5. **Step 1:** Update $w_{b,m}$ and β_b .
6. **Step 2:** Compute $\|w_{b,m}\|_{\mathcal{H}_m}^2$.
7. Update $\theta_{b,m}$.
8. **Step 3:** **For** $k = 1, 2, \dots$ **do**
9. $z^k = \mu^k - \eta \partial l(\mu^k)$.
10. $y^k = \sum \text{prox}_{\eta h}(z^k)$.
11. $\mu^{k+1} = y^k + \frac{k-1}{k+2}(y^k - y^{k-1})$.
12. **End For**
13. **End For**
14. **End While**
15. Output ω .

*SHL training attempts to minimize the normalized (by B) expected Hamming distance of a labeled sample to the correct codeword, which is demonstrated next. We constrain ourselves to the case, where the training set consists only of labeled samples (i.e., $N = \mathcal{N}_L, \mathcal{N}_U = 0$) and, for reasons of convenience, to our single codeword *SHL. The definitions of the MKL hypothesis space for *SHL can be found in Sec. 3. Before we provide the generalization results, the following two definitions are necessary.

Definition 1. A Random Variable (RV) σ that is Bernoulli distributed such that $\Pr\{\sigma = \pm 1\} = \frac{1}{2}$ will be called a Rademacher RV.

Definition 2. Let $\mathcal{G} \triangleq \{g : \mathcal{Z} \mapsto \mathbb{R}\}$ be a set of functions of an arbitrary domain \mathcal{Z} and $Q = \{z_n\}_{n=1}^N$ a set of iid samples from \mathcal{Z} according to a distribution D . Then, the Empirical Rademacher Complexity (ERG) of \mathcal{G} w.r.t Q is defined as:

$$\widehat{\mathfrak{R}}_Q(\mathcal{G}) \triangleq \mathbb{E}_\sigma \left\{ \sup_{g \in \mathcal{G}} \frac{1}{N} \sum_{n=1}^N \sigma_n g(z_n) \mid Q \right\} \quad (14)$$

where $\mathbb{E}_\sigma \{\cdot\} \triangleq \mathbb{E}_{\sigma_1} \{\mathbb{E}_{\sigma_2} \{\dots \mathbb{E}_{\sigma_N} \{\cdot\} \dots\}\}$ and $\{\sigma_n\}_{n=1}^N$ are iid Rademacher RV. In the rest of the section, the condition on Q will be omitted for simplicity. Additionally, the Rademacher Complexity (RC) of \mathcal{G} for a sample size N is defined as:

$$\mathfrak{R}_N(\mathcal{G}) \triangleq \mathbb{E}_{Q \sim D^N} \left\{ \widehat{\mathfrak{R}}_Q(\mathcal{G}) \right\} \quad (15)$$

We also need the following two lemmas before showing our final concentration results.

Lemma 1. Let \mathcal{Z} be an arbitrary set, $\tilde{\mathcal{F}} \triangleq \{\mathbf{f} : z \mapsto \mathbf{f}(z) \in \mathbb{R}^B, z \in \mathcal{Z}\}$, $\Psi : \mathbb{R}^B \rightarrow \mathbb{R}$ be L -Lipschitz continuous w.r.t $\|\cdot\|_1$. Also, define $\Psi \circ \tilde{\mathcal{F}} \triangleq \{g : z \mapsto \Psi(\mathbf{f}(z))\}$ and $\|\tilde{\mathcal{F}}\|_1 \triangleq \{h : z \mapsto \|\mathbf{f}(z)\|_1, \mathbf{f} \in \tilde{\mathcal{F}}\}$ then

$$\widehat{\mathfrak{R}}_Q(\Psi \circ \tilde{\mathcal{F}}) \leq L \widehat{\mathfrak{R}}_Q(\|\tilde{\mathcal{F}}\|_1) \quad (16)$$

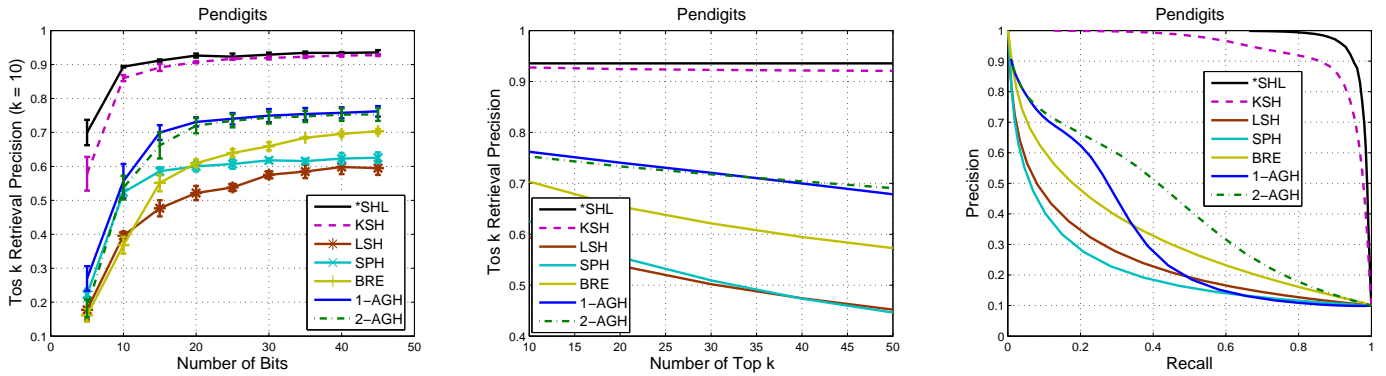


Fig. 1. The top k retrieval results and Precision-Recall curve on *Pendigits* dataset over *SHL and 6 other hashing algorithms. (view in color)

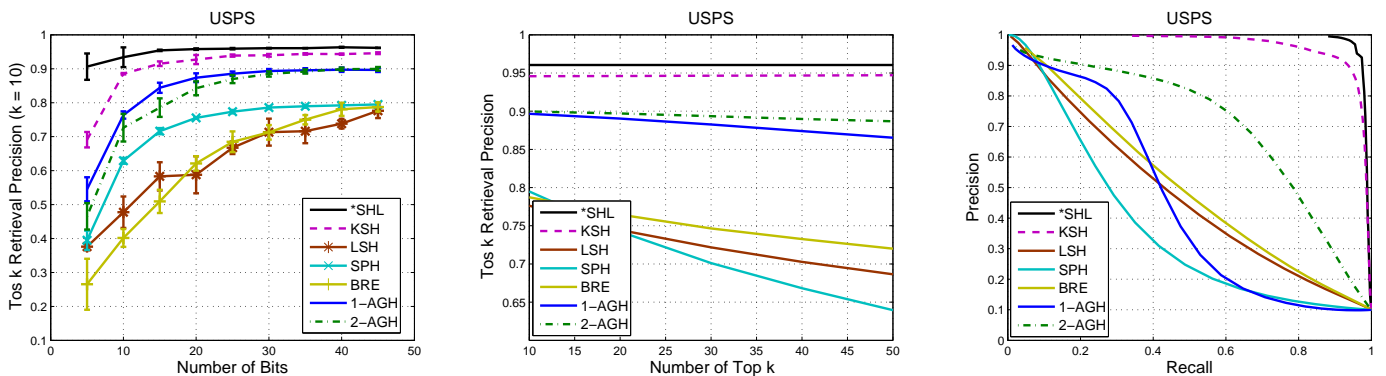


Fig. 2. The top k retrieval results and Precision-Recall curve on *USPS* dataset over *SHL and 6 other hashing algorithms. (view in color)

where Q is a set of N samples drawn from \mathcal{Z} .

Lemma 2. Let \mathcal{Z} be an arbitrary set. Define: $\tilde{\mathcal{F}} \triangleq \{\mathbf{f} : z \mapsto \mathbf{f}(z) \in \mathbb{R}^B, z \in \mathcal{Z}, \|\tilde{\mathcal{F}}\|_1 \triangleq \{h : z \mapsto \|\mathbf{f}(z)\|_1, \mathbf{f} \in \tilde{\mathcal{F}}\}$ and $\mathbf{1}^T \tilde{\mathcal{F}} \triangleq \{g : z \mapsto \mathbf{1}^T \mathbf{f}(z), \mathbf{f} \in \tilde{\mathcal{F}}\}$. Let's further assume that if $\mathbf{f}(z) \triangleq [f_1(z), \dots, f_B(z)]^T \in \tilde{\mathcal{F}}$ for $z \in \mathcal{Z}$, then also $[\pm f_1(z), \dots, \pm f_B(z)] \in \tilde{\mathcal{F}}$ for any combination of signs. Then:

$$\hat{\mathcal{R}}_Q(\|\tilde{\mathcal{F}}\|_1) \leq \hat{\mathcal{R}}_Q(\mathbf{1}^T \tilde{\mathcal{F}}) \quad (17)$$

where Q is a set of N samples drawn from \mathcal{Z} .

The detailed proof is provided in Appendix C for Lemma 1 and in Appendix D for Lemma 2.

To show the main theoretical result of our paper with the help of the previous lemmas, we will consider the sets of functions

$$\bar{\mathcal{F}} \triangleq \{\mathbf{f} : x \mapsto [f_1(x), \dots, f_B(x)]^T, f_b \in \mathcal{F}, b \in \mathbb{N}_B\} \quad (18)$$

$$\mathcal{F} \triangleq \{f : x \mapsto \langle w, \phi_\theta(x) \rangle_{\mathcal{H}_\theta} + \beta, \beta \in \mathbb{R}, w \in \Omega_w(\theta), \theta \in \Omega_\theta\} \quad (19)$$

where $\Omega_w(\theta) \triangleq \{w \in \mathcal{H}_\theta : \|w\|_{\mathcal{H}_\theta} \leq R\}$ for some $R \geq 0$ and $\Omega_\theta \triangleq \{\theta \in \mathbb{R}^M : \theta \succeq \mathbf{0}, \|\theta\|_p \leq 1\}$ for some $p \geq 1$.

Theorem 3. Assume reproducing kernels of $\{\mathcal{H}_m\}_{m=1}^M$ s.t. $k_m(x, x') \leq r^2, \forall x, x' \in \mathcal{X}$ and a set Q of iid samples $Q = \{(x_1, l_1), \dots, (x_N, l_N)\}$. Then for $\rho > 0$ independent of Q , for any $\mathbf{f} \in \bar{\mathcal{F}}$, any $\mu \in \mathcal{M}$, where $\mathcal{M} \triangleq \{\mu : \mathbb{N}_C \rightarrow \mathbb{H}^B\}$ and any $0 < \delta < 1$, with probability $1 - \delta$, it holds that:

$$er(\mathbf{f}, \mu) \leq \hat{er}(\mathbf{f}, \mu) + \frac{2R}{\rho} \sqrt{rM^{\frac{1}{p'}}} \sqrt{\frac{p'}{N^3}} + \sqrt{\frac{\log(\frac{1}{\delta})}{2N}} \quad (20)$$

where $er(\mathbf{f}, \mu) \triangleq \frac{1}{B} \mathbb{E}\{d(\text{sgn } \mathbf{f}(x), \mu(l))\}$, $l \in \mathbb{N}_C$ is the true label of $x \in \mathcal{X}$, $\hat{er}(\mathbf{f}, \mu_l) \triangleq \frac{1}{N_B} \sum_{n,b} \Phi_\rho(f_b(x_n) \mu_{n,b})$, where $\Phi_\rho(u) \triangleq \min\{1, \max\{0, 1 - \frac{u}{\rho}\}\}$ and $p' \triangleq \frac{p}{p-1}$.

The detailed proofs for Theorem 3 can be found in Appendix E.

6 EXPERIMENTS

6.1 Supervised Hash Learning Results

In this section, we compare *SHL to other state-of-the-art hashing algorithms:

- Kernel Supervised Learning (KSH)³ [22].

3. <http://www.ee.columbia.edu/ln/dvmm/downloads/WeiKSHCode/dlfc>

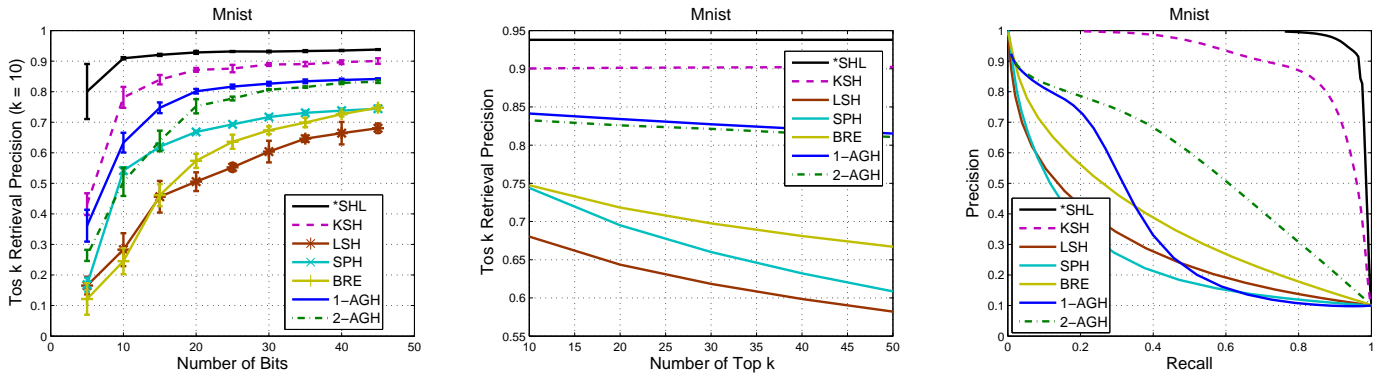


Fig. 3. The top k retrieval results and Precision-Recall curve on *Mnist* dataset over *SHL and 6 other hashing algorithms. (view in color)

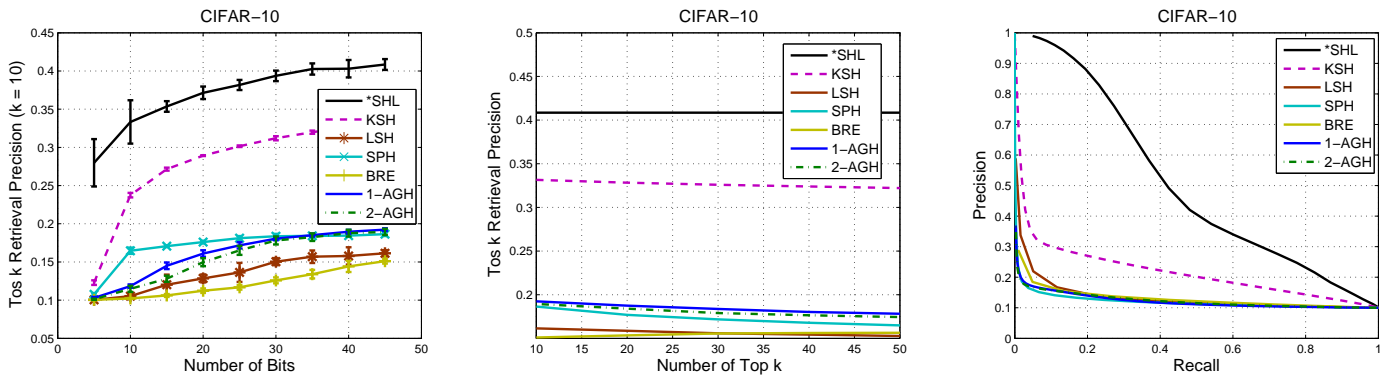


Fig. 4. The top k retrieval results and Precision-Recall curve on *CIFAR-10* dataset over *SHL and 6 other hashing algorithms. (view in color)

- Binary Reconstructive Embedding (BRE)⁴ [13].
- single-layer Anchor Graph Hashing (1-AGH) and its two-layer version (2-AGH)⁵ [29].
- Spectral Hashing (SPH)⁶ [27].
- Locality-Sensitive Hashing (LSH) [9].

Five datasets, which are widely utilized in other hashing papers as benchmarks, were considered:

- *Pendigits*: a digit dataset (10,992 samples, 256 features, 10 classes) of 44 writers from the *UCI Repository*⁷. In our experiment, we randomly choose 3,000 for training and the rest for testing.
- *USPS*: a digit dataset also from the *UCI Repository*, is numeric data from the scanning of handwritten digits from envelopes by the U.S. Postal Service. Among the dataset (9,298 samples, 256 features, 10 classes), 3000 were used for training and others for testing.
- *Mnist*⁸: a hand written digit dataset which contains 70,000 samples, 784 features and 10 classes. The digits have been size-normalized and centered. In

our experiment, 6,000 for training and 64,000 for testing.

- *CIFAR-10*⁹: a labeled image dataset collected from 80 million tiny images¹⁰. The dataset consists of 60,000 samples, 1,024 features, 10 classes. We use 6,000 for training and the rest for testing.
- *PASCAL07*¹¹ [48]: a dataset contains annotated consumer photographs collected from the flickr photo sharing website. The dataset consists of 6878 samples, 1,024 features after down-sampling the images, 10 classes. Here, 3,000 for training and others for testing.

For all the algorithms used, average performances over 5 runs are reported in terms of the following two criteria: (i) retrieval precision of k -closest hash codes of training samples; we used $k = \{10, 15, \dots, 50\}$. (ii) Precision-Recall (PR) curve, where retrieval precision and recall are computed for hash codes within a Hamming radius of $r \in \mathbb{N}_B$.

The following *SHL settings were used: SVM's parameter λ_1 was set to 1000; for MKL, 11 kernels were considered: 1 normalized linear kernel, 1 normalized polynomial kernel

4. <http://web.cse.ohio-state.edu/~kulis/bre/bre.tar.gz>

5. <http://www.ee.columbia.edu/ln/dvmm/downloads/WeiGraphConstructCode2011/dlform.htm>

6. <http://www.cs.huji.ac.il/~yweiss/SpectralHashing/sh.zip>

7. <http://archive.ics.uci.edu/ml/>

8. <http://yann.lecun.com/exdb/mnist/>

9. <http://www.cs.toronto.edu/~kriz/cifar.html>

10. <http://groups.csail.mit.edu/vision/TinyImages/>

11. <http://pascal11n.ecs.soton.ac.uk/challenges/VOC/>

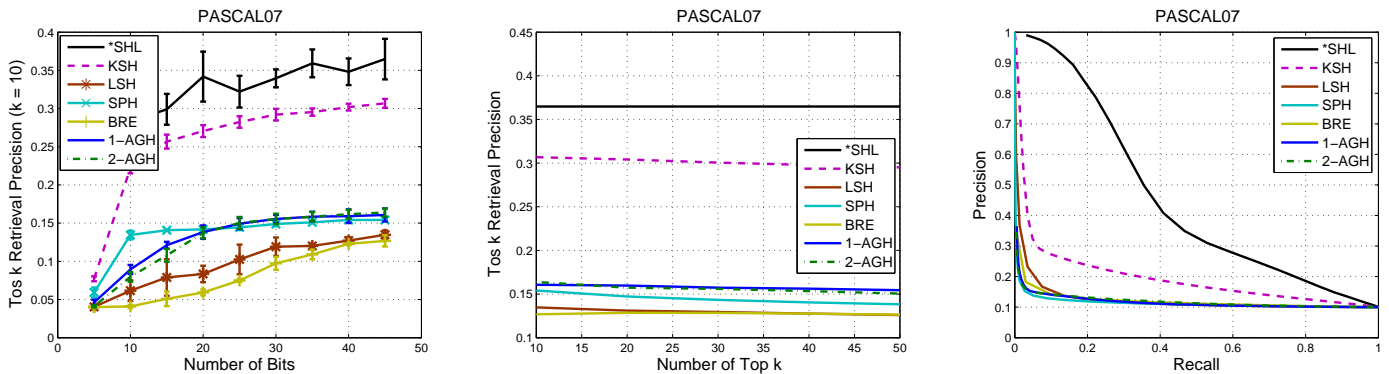


Fig. 5. The top k retrieval results and Precision-Recall curve on *PASCAL07* dataset over *SHL and 6 other hashing algorithms. (view in color)

and 9 Gaussian kernels. For the polynomial kernel, the bias was set to 1.0 and its degree was chosen as 2. For the bandwidth σ of the Gaussian kernels the following values were used: $[2^{-7}, 2^{-5}, 2^{-3}, 2^{-1}, 1, 2^1, 2^3, 2^5, 2^7]$. Regarding the MKL constraint set, a value of $p = 2$ was chosen. λ_2 was set to 2000 for *Pendigits*, *USPS* and *PASCAL07* and $\lambda_2 = 6000$ for the rest of the datasets.

For the remaining approaches, namely KSH, SPH, AGH, BRE, parameter values were used according to recommendations found in their respective references. All obtained results are reported in Fig. 1 through Fig. 5.

We clearly observe that *SHL performs the best among all the algorithms considered. For all the datasets, *SHL achieves the highest top-10 retrieval precision. Especially for non-digits datasets (*CIFAR-10*, *PASCAL07*), *SHL achieves significantly better results. As for the PR-curve, *SHL also obtains the largest areas under the curve. Although impressive results have been reported in [22] for KSH, in our experiments, *SHL outperforms it across all datasets. Moreover, we observe that supervised hash learning algorithms, except BRE, perform better than unsupervised variants. BRE may need a longer bit length to achieve better performance like in Fig. 1 and Fig. 3. Additionally, it is worth mentioning that *SHL performs impressively with short bit length across all the datasets.

AGH also yields good results, compared with other unsupervised hashing algorithms, because it utilizes anchor points as side information to generate hash codes. With the exception of *SHL and KSH, the remaining approaches exhibit poor performance for the non-digits datasets we considered (*CIFAR-10* and *PSACAL07*).

When varying the top- k number between 10 and 50, once again with the exception of *SHL and KSH, the performance of the remaining approaches deteriorated in terms of top- k retrieval precision. KSH performs slightly worse, when s increases, while *SHL's performance remain robust for *CIFAR-10* and *PSACAL07*. It is worth mentioning that the two-layer AGH exhibits better robustness than its single-layer version for datasets involving images of digits. Finally, Fig. 6 and Fig. 7 show some qualitative results for the *CIFAR-10* and *Mnist* datasets. In conclusion, it seems that both *SHL's performances are superior at every code length we

considered.

6.2 Transductive Hash Learning Results

As a proof of concept, in this section, we report a performance comparison of *SHL, when used in an inductive versus a transductive [49] mode. Note that, to the best of our knowledge, apart from our method, there are no other hash learning approaches to date that can accommodate transductive hash learning. For illustration purposes, we used the *Vowel* and *Letter* datasets from *UCI Repository*. We randomly chose 330 training and 220 test samples for the *Vowel* and 300 training and 200 test samples for the *Letter*. Each scenario was run 20 times and the code length (B) varied from 4 to 15 bits. The results are shown in Fig. 8 and reveal the potential merits of the transductive *SHL learning mode across a range of code lengths.

6.3 Image Segmentation

Besides content-based image retrieval, the proposed *SHL can also be utilized in the other applications, for example, the foreground/background interactive image segmentation [50], where the images are partially labeled as foreground and background by users. In *SHL, while foreground and background are represented by two codewords, the rest of the pixels can be labeled in semi-supervised learning scenario. In this section, we show the interactive image segmentation results using *SHL on the dataset introduced in [51]. The hash code length is 5 and the rest of the parameters settings follow the previous section. For each pixel, the RGB values are used as features. The results are shown in Fig. 9. We notice that, provided with partially labeled information, *SHL successfully segment the foreground object from the background. Especially in (e), although all the flower pots share the same color, *SHL only highlight the labeled one and its plant. Additionally, in some images, like (c) and (f), shaded areas fail to be segmented. In these cases, more pixel features may be necessary for better results.

6.4 *SHL for Large Data Set

Large data sets require a huge kernel matrix which can not be fit into the memory of one single machine. Thus,

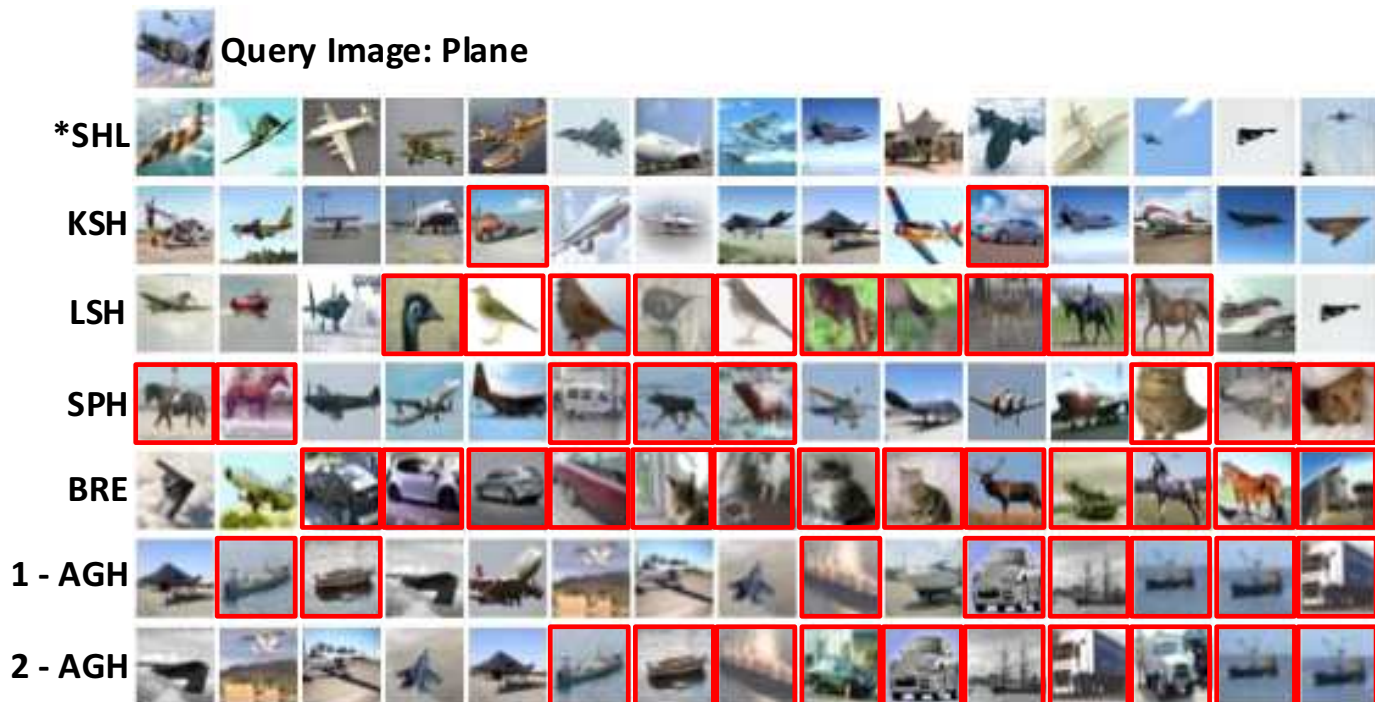


Fig. 6. Qualitative results on CIFAR-10. Query image is "Plane". The remaining 15 images for each row were retrieved using 45-bit binary codes generated by different hashing algorithms. Red box indicates wrong retrieval results.

LIBSKYLARK, a parallel machine learning software which utilizes kernel approximation and ADMM, replaces *LIBSVM* in *SHL. In this section, we created our own clusters in *Amazon Web Service*¹². One cluster consists of 2 nodes while the other one contains 10 nodes. Each node has Xeon E5-2666 CPU and 3.75 GB memory.

Three data sets are considered here:

- *USPS*: with 256 features, 7291 samples are used for training, while 2007 samples are for testing.
- *Mnist*: 60K are for training and 10K are for testing. This data set contains 784 features.
- *Mnist1M*: 784 features. 1 million samples for training and 100K for testing.

*LIBSKYLARK*¹³ is downloaded and compiled. We run the experiments using 5 bits, 25 bits and 45 bits of the codeword for the three data sets. *SHL's parameters are set as the previous sections. The results of running time and top-10 retrieval accuracies are reported in Table 1:

Several observations can be made here: firstly, with the help of *LIBSKYLARK*, our framework *SHL can solve large data sets like *Mnist1M*. As reported in Table 1, *SHL provides competitive retrieval results using about 13 hours for the 45 bits codeword. Secondly, as shown in the second and third row in the table, a larger cluster will benefit more from parallel computing. Here, *Mnist* run on the 10 nodes cluster need almost 25% running time compared with the same data set on a 2 node cluster. Thus, when confronting with even larger data sets, a larger cluster with more powerful nodes can be a solution.

12. <https://aws.amazon.com/>

13. <http://xdata-skylark.github.io/libskylark/>

7 CONCLUSIONS

In this paper we considered a novel hash learning framework, namely *Supervised Hash Learning (*SHL). The method has the following main advantages: first, its Majorization-Minimization (MM)/Block Coordinate Descent (BCD) training algorithm is efficient and simple to implement. Secondly, the framework is able to address supervised, unsupervised or even semi-supervised learning tasks. Additionally, after introducing a regularization over the multiple codewords, we also provide the Proximal Sub-gradient Descent (PSD) method to solve this regularization.

In order to show the merits of the methods, we performed a series of experiments involving 5 benchmark datasets. In experiments that were conducted, a comparison between our methods with the other 6 state-of-the-art hashing methods shows *SHL to be highly competitive. Moreover, we also give results on transductive learning scenario. Additionally, another application based on our framework, interactive image segmentation, is also showcased in the experimental section. Finally, we introduce *SHL can also solve problems containing a huge number of samples.

APPENDIX A PROOF OF PROP. 3

Proof. By replacing hinge function in Prob. (6), we got the following problem for the first block minimization:

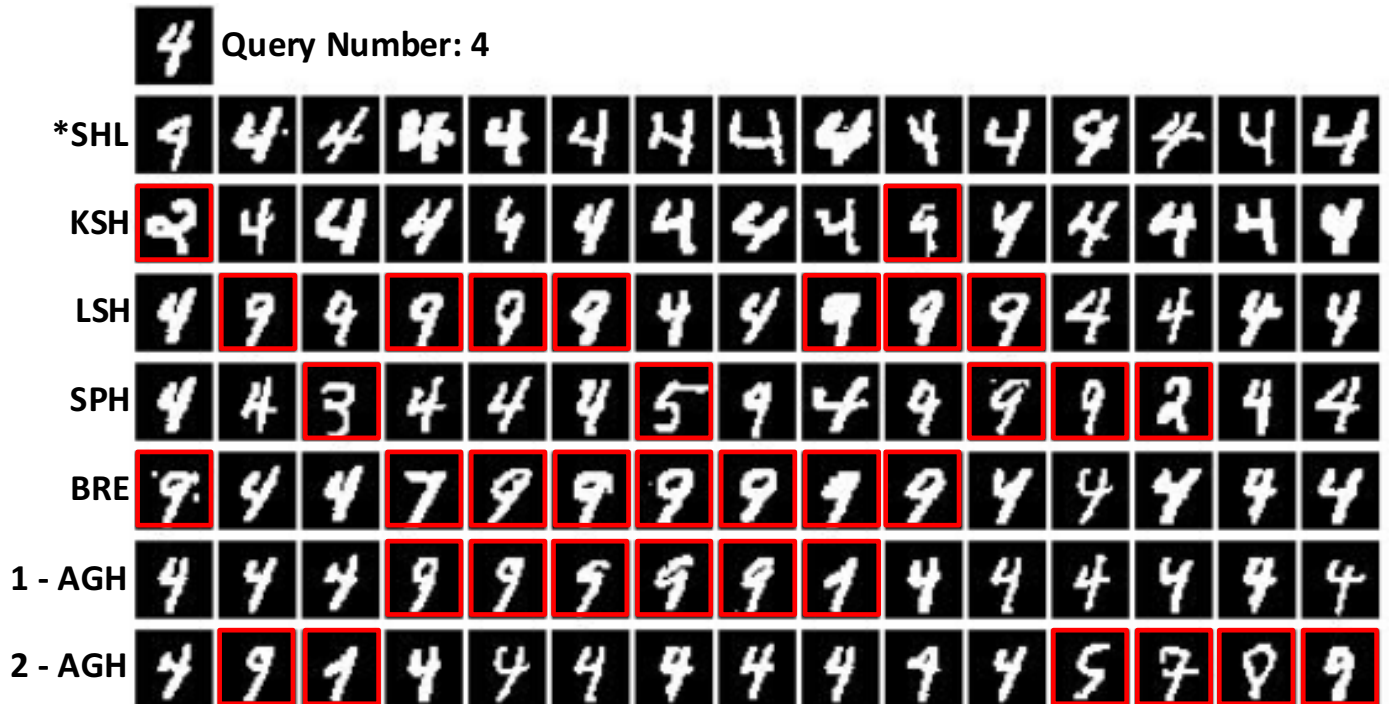


Fig. 7. Qualitative results on Mnist. Query image is "4". The remaining 15 images for each row were retrieved using 45-bit binary codes generated by different hashing algorithms. Red box indicates wrong retrieval results.

TABLE 1

Top-10 retrieval results and running time for *SHL for various data sets. Here, running time secs means seconds, mins means minutes and hours means hours.

DATA SETS	NODES	TRAINING	TESTING	BITS	ACCURACY	TIME
USPS	2	7291	2007	5	0.916	45.82 secs
				25	0.936	227.17 secs / 3.78 mins
				45	0.941	408.66 secs / 6.90 mins
Mnist	2	60K	10K	5	0.826	1690.46 secs / 28.17 mins
				25	0.960	8406.04 secs / 140.08 mins / 2.33 hours
				45	0.969	4253.28 secs / 251.85 mins / 4.20 hours
Mnist	10	60K	10K	5	0.839	487.88 secs / 8.13 mins
				25	0.962	2361.07 secs / 39.35 mins
				45	0.964	4253.28 secs / 70.89 mins / 1.18 hours
Mnist1M	10	1M	100K	5	0.824	7918.38 secs / 131.97 mins / 2.20 hours
				25	0.927	28066.37 secs / 467.77 mins / 7.80 hours
				45	0.934665	48574.96 secs / 809.58 mins / 13.49 hours

$\xi_{c,n,s}^b$'s, $\eta_b \triangleq [\eta_{b,1}, \eta_{b,2}, \dots, \eta_{b,N}]^T \in \mathbb{R}^N$ and $\mu_b \triangleq [\mu_{1,1}^b, \dots, \mu_{1,S}^b, \mu_{2,1}^b, \dots, \mu_{C,S}^b]^T \in \mathbb{R}^{CS}$, the vectorized version of Prob. (21) with Eq. (22):

$$\min_{\substack{w_{b,m}, \beta_b \\ \xi_{c,n,s}^b}} \lambda_1 \sum_c \sum_s \sum_n \gamma'_{c,n,s} \xi_{c,n,s}^b + \frac{1}{2} \sum_m \frac{\|w_{b,m}\|_{\mathcal{H}_m}^2}{\theta_{b,m}}$$

$$\text{s.t. } \xi_{c,n,s}^b \geq 0$$

$$\xi_{c,n,s}^b \geq 1 - \left(\sum_m \langle w_{b,m}, \phi_m(x) \rangle_{\mathcal{H}_m} + \beta_b \right) \mu_{c,s}^b \quad (21)$$

First of all, after considering Representer Theorem [52], we have:

$$w_{b,m} = \theta_{b,m} \sum_n \eta_{b,n} \phi_m(x_n) \quad (22)$$

where n is index of the training samples. By defining $\xi_b \in \mathbb{R}^{NCS}$ to be the vector containing all

$$\min_{\eta_b, \xi_b, \beta_b} \lambda_1 \gamma' \xi_b + \frac{1}{2} \eta_b^T \mathbf{K}_b \eta_b$$

$$\text{s.t. } \xi_b \succeq 0$$

$$\xi_b \succeq \mathbf{1}_{NCS} - (\mu_b \otimes \mathbf{K}_b) \eta_b - (\mu_b \otimes \mathbf{1}_N) \beta_b \quad (23)$$

Where γ' and \mathbf{K}_b are defined in Prop. 3. Take the Lagrangian \mathcal{L} and its derivatives, we have the following relations, here α_b and ζ_b are Lagrangian multipliers for the two constraints:

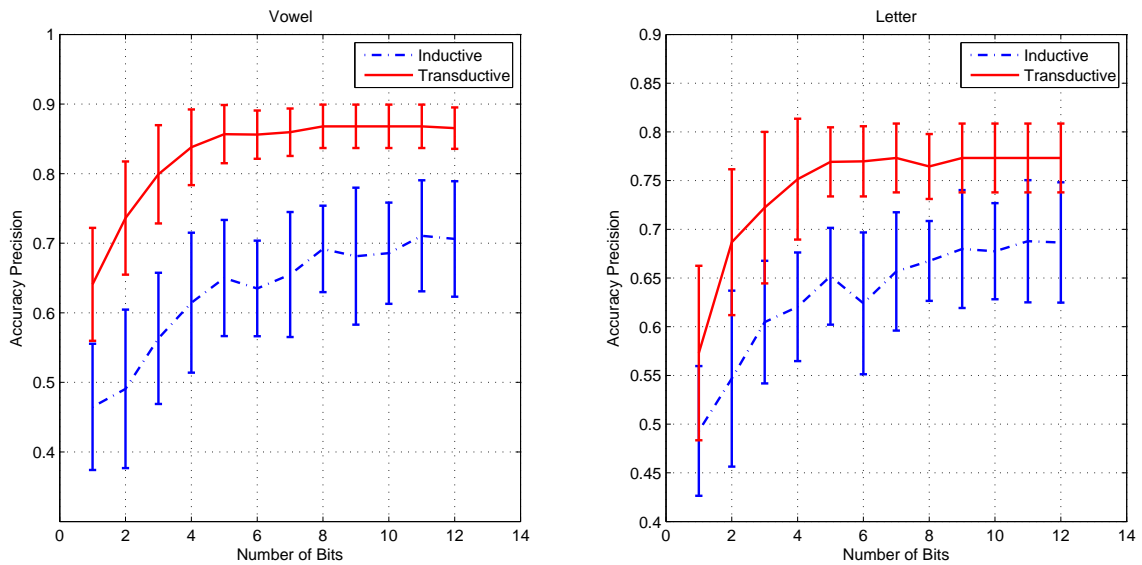


Fig. 8. Accuracy results between Inductive and Transductive Learning.

$$\frac{\partial \mathcal{L}}{\partial \xi_b} = \mathbf{0} \Rightarrow \begin{cases} \zeta_b = \lambda_1 \gamma' - \alpha_b \\ \mathbf{0} \preceq \alpha_b \preceq \lambda_1 \gamma' \end{cases} \quad (24)$$

$$\frac{\partial \mathcal{L}}{\partial \beta_b} = \mathbf{0} \Rightarrow \alpha_b^T (\mu_b \otimes \mathbf{1}_N) = 0 \quad (25)$$

$$\frac{\partial \mathcal{L}}{\partial \eta_b} = \mathbf{0} \stackrel{\exists \mathbf{K}_b^{-1}}{\Rightarrow} \eta_b = \mathbf{K}_b^{-1} (\mu_b \otimes \mathbf{K}_b)^T \alpha_b \quad (26)$$

Substitute Eq. (24), Eq. (25) and Eq. (26) back into \mathcal{L} , meanwhile, we notice the quadratic term becomes:

$$\begin{aligned} & (\mu_b \otimes \mathbf{K}_b) \mathbf{K}_b^{-1} (\mu_b^T \otimes \mathbf{K}_b) \\ &= (\mu_b \otimes \mathbf{K}_b) (\mathbf{1} \otimes \mathbf{K}_b^{-1}) (\mu_b^T \otimes \mathbf{K}_b) \\ &= (\mu_b \otimes \mathbf{I}_{N \times N}) (\mu_b^T \otimes \mathbf{K}_b) \\ &= (\mu_b \mu_b^T) \otimes \mathbf{K}_b \end{aligned} \quad (27)$$

Eq. (27) can be further derived:

$$\begin{aligned} & (\mu_b \mu_b^T) \otimes \mathbf{K}_b \\ &= [(\text{diag}(\mu_b) \mathbf{1}_C) (\text{diag}(\mu_b) \mathbf{1}_C)^T] \otimes \mathbf{K}_b \\ &= [\text{diag}(\mu_b) (\mathbf{1}_C \mathbf{1}_C^T) \text{diag}(\mu_b)] \otimes [\mathbf{I}_N \mathbf{K}_b \mathbf{I}_N] \\ &= [\text{diag}(\mu_b) \otimes \mathbf{I}_N] [(\mathbf{1}_C \mathbf{1}_C^T) \otimes \mathbf{K}_b] [\text{diag}(\mu_b) \otimes \mathbf{I}_N] \\ &= [\text{diag}(\mu_b \otimes \mathbf{1}_N)] [(\mathbf{1}_C \mathbf{1}_C^T) \otimes \mathbf{K}_b] [\text{diag}(\mu_b \otimes \mathbf{1}_N)] \\ &= \mathbf{D}_b [(\mathbf{1}_C \mathbf{1}_C^T) \otimes \mathbf{K}_b] \mathbf{D}_b \end{aligned} \quad (28)$$

The first equality comes from $\text{diag}(\mathbf{u}) \mathbf{1} = \mathbf{u}$ for some vector \mathbf{u} . The third equality is the mixed-product property of Kronecker product. This relation $\text{diag}(\mathbf{u} \otimes \mathbf{1}) = \text{diag}(\mathbf{u}) \otimes \mathbf{I}$ gives the fourth equality. \mathbf{D}_b is defined in Prop. 3.

After considering Eq. (27) and Eq. (28), we get the final dual form as shown in Prop. 3. \square

APPENDIX B PROOF OF PROP. 4

Proof. With the definitions of proximal operator Eq. (11), we have the following problem to minimize over:

$$\begin{aligned} P(\mu) &= \eta \|U\mu\|_2 + \frac{1}{2} \|\mathbf{v} - \mu\|_2^2 \\ &= \eta \|U\mu\|_2 + \frac{1}{2} \|\mathbf{v}_1 - \mu_1\|_2^2 + \cdots + \frac{1}{2} \|\mathbf{v}_S - \mu_S\|_2^2 \end{aligned} \quad (29)$$

The second equality follows from the definitions of the vectors μ and \mathbf{v} . Since L_2 norm is non differentiable at point 0, we optimize Eq. (29) in two cases.

Case 1: when $\mu_i \neq \mu_j$, we take the gradients for each individual μ_1 to μ_S :

$$\begin{cases} \frac{\partial P(\mu)}{\partial \mu_1} = \mu_1 - \mathbf{v}_1 = \mathbf{0} \\ \vdots \\ \frac{\partial P(\mu)}{\partial \mu_i} = \eta \frac{\mu_i - \mu_j}{\|\mu_i - \mu_j\|_2} + \mu_i - \mathbf{v}_i = \mathbf{0} \\ \vdots \\ \frac{\partial P(\mu)}{\partial \mu_j} = \eta \frac{\mu_j - \mu_i}{\|\mu_i - \mu_j\|_2} + \mu_j - \mathbf{v}_j = \mathbf{0} \\ \vdots \\ \frac{\partial P(\mu)}{\partial \mu_S} = \mu_S - \mathbf{v}_S = \mathbf{0} \end{cases} \quad (30)$$

Solve the linear equations with μ_i and μ_j :

$$\begin{cases} \mu_i = \frac{1}{2\tau+1} [(1+\tau)\mathbf{v}_i + \tau\mathbf{v}_j] \\ \mu_j = \frac{1}{2\tau+1} [\tau\mathbf{v}_i + (1+\tau)\mathbf{v}_j] \end{cases} \quad (31)$$

where $\tau \triangleq \eta/\delta$ and $\delta \triangleq \|\mu_i - \mu_j\|_2$. Now we have the following derivations:

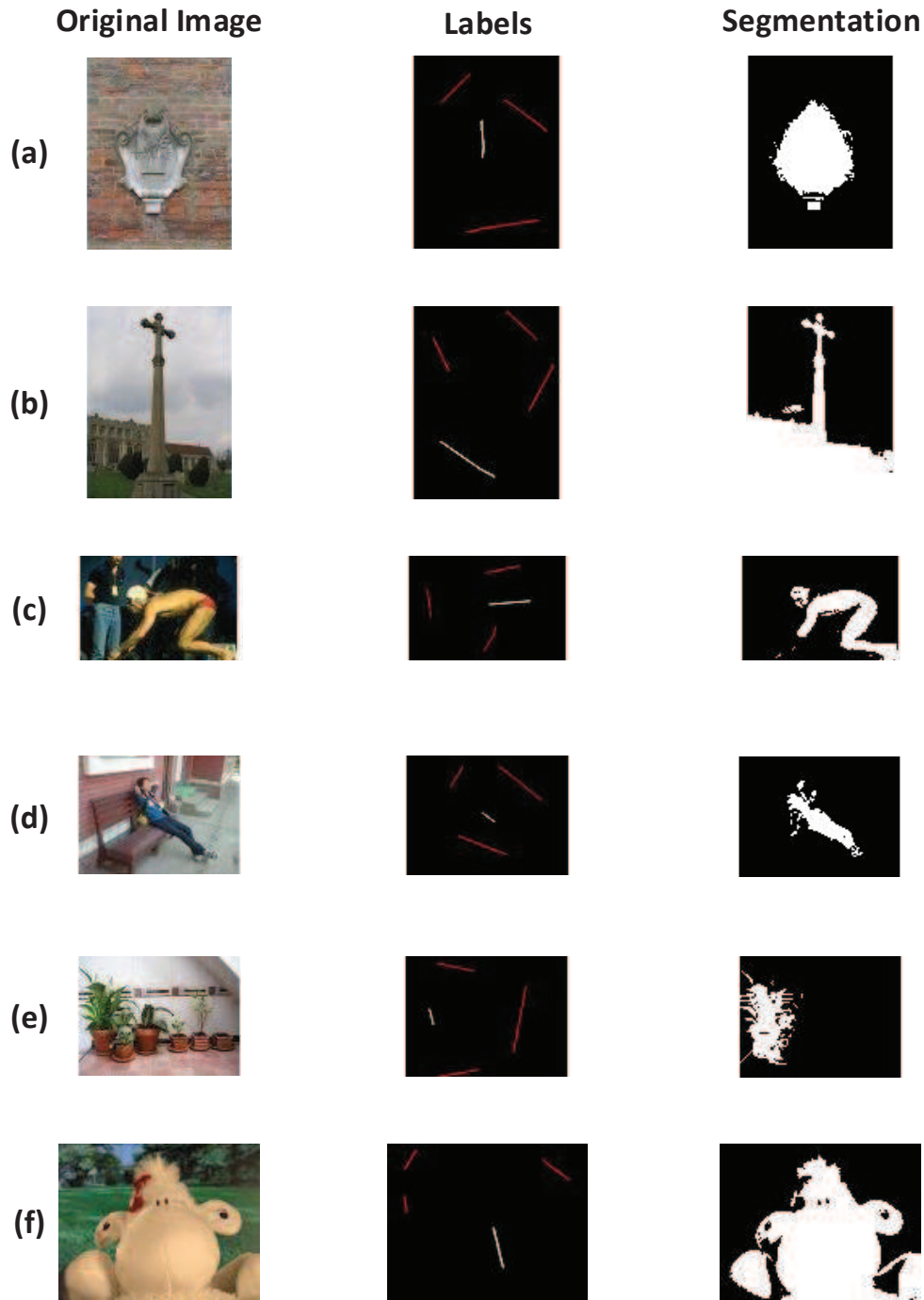


Fig. 9. Foreground/Background interactive image segmentation. The left column contains the original images. The middle column includes labeled pixels. The right column shows the results of the segmentation on.

$$\begin{aligned}
 \mu_i - \mu_j &= \frac{1}{2\tau + 1}(\mathbf{v}_i - \mathbf{v}_j) \\
 \Rightarrow \|\mu_i - \mu_j\|_2 &= \frac{1}{2\tau + 1} \|\mathbf{v}_i - \mathbf{v}_j\|_2 \\
 \Rightarrow \delta &= \frac{\|\mathbf{v}_i - \mathbf{v}_j\|_2}{2\eta + 1} \\
 \Rightarrow \delta &= \|\mu_i - \mu_j\|_2 = \|\mathbf{v}_i - \mathbf{v}_j\|_2 - 2\eta
 \end{aligned} \quad (32)$$

Plug τ and Eq. (32) into Eq. (31), we achieve the results for

μ_i and μ_j :

$$\begin{cases} \mu_i = \alpha_1 \mathbf{v}_i + \alpha_2 \mathbf{v}_j \\ \mu_j = \alpha_2 \mathbf{v}_i + \alpha_1 \mathbf{v}_j \end{cases} \quad (33)$$

Here $\alpha_1 = 1 - \alpha_2$ and $\alpha_2 = \frac{\eta}{\|\mathbf{v}_i - \mathbf{v}_j\|_2}$. Additionally, Eq. (32) is larger than 0 which gives the following condition for **Case 1**: $0 < \eta \leq \frac{\|\mathbf{v}_i - \mathbf{v}_j\|_2}{2}$.

Case 2: when $\mu_i = \mu_j$, μ_i and μ_j are represented as:

$$\begin{cases} \boldsymbol{\mu}_i = \frac{1}{2}\mathbf{v}_i + \frac{1}{2}\mathbf{v}_j \\ \boldsymbol{\mu}_j = \frac{1}{2}\mathbf{v}_i + \frac{1}{2}\mathbf{v}_j \end{cases} \quad (34)$$

Note that this case satisfies when $\eta > \frac{\|\mathbf{v}_i - \mathbf{v}_j\|_2}{2}$.

Combining two cases, the results provided in Prop. 4 are achieved. \square

APPENDIX C PROOF OF LEMMA 1

Proof. From Definition 2, we have:

$$\begin{aligned} \widehat{\mathfrak{R}}_Q(\Psi \circ \widetilde{\mathcal{F}}) &= \frac{1}{N} \mathbb{E}_\sigma \left\{ \sup_{\mathbf{f} \in \widetilde{\mathcal{F}}} \sum_n \sigma_n \Psi(\mathbf{f}(z_n)) \right\} = \\ &= \frac{1}{N} \mathbb{E}_{\sigma_{N-1}} \left\{ \mathbb{E}_{\sigma_N} \left\{ \sup_{\mathbf{f} \in \widetilde{\mathcal{F}}} [u(\mathbf{f}) + \sigma_N \Psi(\mathbf{f}(z_N))] \right\} \right\} \\ &= \frac{1}{N} \mathbb{E}_{\sigma_{N-1}} \{A(\sigma_{N-1})\} \end{aligned} \quad (35)$$

where $u(\mathbf{f}) \triangleq \sum_{n=1}^{N-1} \sigma_n \Psi(\mathbf{f}(z_n))$ and $A(\sigma_{N-1}) \triangleq \mathbb{E}_{\sigma_N} \left\{ \sup_{\mathbf{f} \in \widetilde{\mathcal{F}}} [u(\mathbf{f}) + \sigma_N \Psi(\mathbf{f}(z_N))] \right\}$.

Expanding the expectation, we get:

$$\begin{aligned} A(\sigma_{N-1}) &= \frac{1}{2} \left[\sup_{\mathbf{f} \in \widetilde{\mathcal{F}}} [u(\mathbf{f}) + \Psi(\mathbf{f}(z_N))] \right. \\ &\quad \left. + \sup_{\mathbf{f} \in \widetilde{\mathcal{F}}} [u(\mathbf{f}) - \Psi(\mathbf{f}(z_N))] \right] \end{aligned} \quad (36)$$

Additionally, we define the following: $\widehat{B}(\mathbf{f}) \triangleq u(\mathbf{f}) + \Psi(\mathbf{f}(z_N))$ and $\widetilde{B}(\mathbf{f}) \triangleq u(\mathbf{f}) - \Psi(\mathbf{f}(z_N))$.

From the superior's definition, we have that $\forall \epsilon > 0$, there are $\widehat{\mathbf{f}}$ and $\widetilde{\mathbf{f}}$ in $\widetilde{\mathcal{F}}$ such that:

$$\sup_{\mathbf{f} \in \widetilde{\mathcal{F}}} \widehat{B}(\mathbf{f}) \geq \widehat{B}(\widehat{\mathbf{f}}) \geq (1 - \epsilon) \sup_{\mathbf{f} \in \widetilde{\mathcal{F}}} \widehat{B}(\mathbf{f}) \quad (37)$$

$$\sup_{\mathbf{f} \in \widetilde{\mathcal{F}}} \widetilde{B}(\mathbf{f}) \geq \widetilde{B}(\widetilde{\mathbf{f}}) \geq (1 - \epsilon) \sup_{\mathbf{f} \in \widetilde{\mathcal{F}}} \widetilde{B}(\mathbf{f}) \quad (38)$$

From Eq. (37) and Eq. (38), for any $\epsilon > 0$, we have:

$$\begin{aligned} (1 - \epsilon)A(\sigma_{N-1}) &\leq \frac{1}{2} \left[\widehat{B}(\widehat{\mathbf{f}}) + \widetilde{B}(\widetilde{\mathbf{f}}) \right] = \\ &= \frac{1}{2} \left[u(\widehat{\mathbf{f}}) + u(\widetilde{\mathbf{f}}) + \Psi(\widehat{\mathbf{f}}(z_N)) - \Psi(\widetilde{\mathbf{f}}(z_N)) \right] \end{aligned} \quad (39)$$

Since Ψ is L -Lipschitz continuous w.r.t the $\|\cdot\|_1$ norm, it holds that:

$$\begin{aligned} \Psi(\widehat{\mathbf{f}}(z_N)) - \Psi(\widetilde{\mathbf{f}}(z_N)) &\leq L \left\| \widehat{\mathbf{f}}(z_N) - \widetilde{\mathbf{f}}(z_N) \right\|_1 = \\ &= L \sum_{b=1}^B |\widehat{f}_b(z_N) - \widetilde{f}_b(z_N)| = \\ &= L \sum_{b=1}^B q_b \left(\widehat{f}_b(z_N) - \widetilde{f}_b(z_N) \right) \end{aligned} \quad (40)$$

where $q_b \triangleq \text{sgn}(\widehat{f}_b(z_N) - \widetilde{f}_b(z_N))$. From Eq. (39) and Eq. (40), we obtain:

$$\begin{aligned} &(1 - \epsilon)A(\sigma_{N-1}) \\ &\leq \frac{1}{2} \left[u(\widehat{\mathbf{f}}) + u(\widetilde{\mathbf{f}}) + L \sum_{b=1}^B q_b \left(\widehat{f}_b(z_N) - \widetilde{f}_b(z_N) \right) \right] = \\ &= \frac{1}{2} \left[\left[u(\widehat{\mathbf{f}}) + L \sum_{b=1}^B q_b \widehat{f}_b(z_N) \right] + \left[u(\widetilde{\mathbf{f}}) - L \sum_{b=1}^B q_b \widetilde{f}_b(z_N) \right] \right] \end{aligned} \quad (41)$$

By the definition of superior, Eq. (41) is bounded by:

$$\begin{aligned} (41) &\leq \sup_{\mathbf{q} \in \mathbb{H}^B} \frac{1}{2} \left[\left[u(\widehat{\mathbf{f}}) + L \sum_b q_b \widehat{f}_b(z_N) \right] + \left[u(\widetilde{\mathbf{f}}) \right. \right. \\ &\quad \left. \left. - L \sum_b q_b \widetilde{f}_b(z_N) \right] \right] \leq \\ &\leq \frac{1}{2} \left[\sup_{\mathbf{q} \in \mathbb{H}^B} \left[u(\widehat{\mathbf{f}}) + L \sum_b q_b \widehat{f}_b(z_N) \right] + \sup_{\mathbf{q} \in \mathbb{H}^B} \left[u(\widetilde{\mathbf{f}}) \right. \right. \\ &\quad \left. \left. - L \sum_b q_b \widetilde{f}_b(z_N) \right] \right] \end{aligned} \quad (42)$$

With the help of Eq. (37) and Eq. (38), Eq. (42) is bounded:

$$\begin{aligned} (42) &\leq \frac{1}{2} \left[\sup_{\mathbf{q} \in \mathbb{H}^B} \sup_{\mathbf{f} \in \widetilde{\mathcal{F}}} \left[u(\mathbf{f}) + L \sum_b q_b f_b(z_N) \right] + \right. \\ &\quad \left. \sup_{\mathbf{q} \in \mathbb{H}^B} \sup_{\mathbf{f} \in \widetilde{\mathcal{F}}} \left[u(\mathbf{f}) - L \sum_b q_b f_b(z_N) \right] \right] = \\ &= \mathbb{E}_{\sigma_N} \left\{ \sup_{\mathbf{q} \in \mathbb{H}^B} \sup_{\mathbf{f} \in \widetilde{\mathcal{F}}} \left[u(\mathbf{f}) + \sigma_N L \sum_b q_b f_b(z_N) \right] \right\} = \\ &= \mathbb{E}_{\sigma_N} \left\{ \sup_{\mathbf{f} \in \widetilde{\mathcal{F}}} \left[u(\mathbf{f}) + \sigma_N L \sup_{\mathbf{q} \in \mathbb{H}^B} \sum_b q_b f_b(z_N) \right] \right\} = \\ &= \mathbb{E}_{\sigma_N} \left\{ \sup_{\mathbf{f} \in \widetilde{\mathcal{F}}} \left[u(\mathbf{f}) + \sigma_N L \sum_b \sup_{q_b \in \{\pm 1\}} q_b f_b(z_N) \right] \right\} = \\ &= \mathbb{E}_{\sigma_N} \left\{ \sup_{\mathbf{f} \in \widetilde{\mathcal{F}}} \left[u(\mathbf{f}) + \sigma_N L \sum_b \text{sgn}(f_b(z_N)) f_b(z_N) \right] \right\} = \\ &= \mathbb{E}_{\sigma_N} \left\{ \sup_{\mathbf{f} \in \widetilde{\mathcal{F}}} \left[u(\mathbf{f}) + \sigma_N L \|\mathbf{f}(z_N)\|_1 \right] \right\} \end{aligned} \quad (43)$$

Since Eq. (43) holds for every $\epsilon > 0$, we have that :

$$A(\sigma_{N-1}) \leq \mathbb{E}_{\sigma_N} \left\{ \sup_{\mathbf{f} \in \widetilde{\mathcal{F}}} \left[u(\mathbf{f}) + \sigma_N L \|\mathbf{f}(z_N)\|_1 \right] \right\} \quad (44)$$

Repeating this process for the remaining σ eventually yields the result of this lemma. \square

APPENDIX D

PROOF OF LEMMA 2

Proof. Let $\Psi(\cdot) \triangleq \|\cdot\|_1$. Utilizing the similar technique in Lemma 1, by defining $u(\mathbf{f}) \triangleq \sum_{n=1}^{N-1} \sigma_n \Psi(\mathbf{f}(z_N))$, we have:

$$\widehat{\mathfrak{R}}_Q(\|\widehat{\mathcal{F}}\|_1) = \frac{1}{N} \mathbb{E}_{\sigma_{N-1}} \{A(\sigma_{N-1})\} \quad (45)$$

Here $A(\sigma_{N-1}) = \mathbb{E}_{\sigma_N} \left\{ \sup_{\mathbf{f} \in \widehat{\mathcal{F}}} [u(\mathbf{f}) + \sigma_N \Psi(\mathbf{f}(z_N))] \right\}$. Similarly, by defining $\widehat{B}(\mathbf{f}) \triangleq u(\mathbf{f}) + \Psi(\mathbf{f}(z_N))$ and $\widetilde{B}(\mathbf{f}) \triangleq u(\mathbf{f}) - \Psi(\mathbf{f}(z_N))$, we have for any $\epsilon > 0$:

$$\begin{aligned} (1 - \epsilon)A(\sigma_{N-1}) &\leq \frac{1}{2} [\widehat{B}(\widehat{\mathbf{f}}) + \widetilde{B}(\widetilde{\mathbf{f}})] = \\ &= \frac{1}{2} [u(\widehat{\mathbf{f}}) + u(\widetilde{\mathbf{f}}) + \Psi(\widehat{\mathbf{f}}(z_N)) - \Psi(\widetilde{\mathbf{f}}(z_N))] \end{aligned} \quad (46)$$

By the reverse triangle inequality and $|\cdot|$'s 1-Lipschitz property:

$$\begin{aligned} \Psi(\widehat{\mathbf{f}}(z_N)) - \Psi(\widetilde{\mathbf{f}}(z_N)) &= \sum_{b=1}^B [|\widehat{f}_b(z_N)| - |\widetilde{f}_b(z_N)|] \leq \\ &\leq \sum_{b=1}^B \text{sgn}(\widehat{f}_b(z_N) - \widetilde{f}_b(z_N)) (\widehat{f}_b(z_N) - \widetilde{f}_b(z_N)) \end{aligned} \quad (47)$$

With the definition of $q_b \triangleq \text{sgn}(\widehat{f}_b(z_N) - \widetilde{f}_b(z_N))$, we combine Eq. (46) and Eq. (47):

$$\begin{aligned} (1 - \epsilon)A(\sigma_{N-1}) &\leq \frac{1}{2} \left[u(\widehat{\mathbf{f}}) + u(\widetilde{\mathbf{f}}) + \sum_{b=1}^B q_b (\widehat{f}_b(z_N) - \widetilde{f}_b(z_N)) \right] = \\ &= \frac{1}{2} \left[\left[u(\widehat{\mathbf{f}}) + \sum_{b=1}^B q_b \widehat{f}_b(z_N) \right] + \left[u(\widetilde{\mathbf{f}}) - \sum_{b=1}^B q_b \widetilde{f}_b(z_N) \right] \right] \end{aligned} \quad (48)$$

For $b \in \mathbb{H}_B$, define $q'_b \triangleq q_b$ if $q_b \neq 0$ and $q'_b \triangleq 1$ otherwise. Also, define $\widehat{f}'(\cdot) \triangleq q'_b \widehat{f}(\cdot)$, then we have $\widehat{f}(\cdot) = q'_b \widehat{f}'(\cdot)$ and :

$$\begin{aligned} u(\widehat{\mathbf{f}}) + \sum_{b=1}^B q_b \widehat{f}_b(z_N) &= \\ &= u(q'_1 \widehat{f}'_1(\cdot), \dots, q'_B \widehat{f}'_B(\cdot)) + \sum_{b=1}^B \widehat{f}'_b(z_N) = \\ &= \sum_{n=1}^{N-1} \sigma_n \sum_{b=1}^B |q'_b \widehat{f}'_b(z_n)| + \sum_{b=1}^B \widehat{f}'_b(z_N) = \\ &= u(\widehat{\mathbf{f}}') + \sum_{b=1}^B \widehat{f}'_b(z_N) \leq \sup_{\mathbf{f} \in \widehat{\mathcal{F}}} \left[u(\mathbf{f}) + \sum_{b=1}^B f_b(z_N) \right] \end{aligned} \quad (49)$$

The above derivation is based on the fact that if $[f_1(z), \dots, f_B(z)]^T \in \widehat{\mathcal{F}}$, then we also have $[\pm f_1(z), \dots, f_B(z)]^T \in \widehat{\mathcal{F}}$ for $z \in \mathcal{Z}$.

Using a similar rationale, we can show that:

$$u(\widetilde{\mathbf{f}}) - \sum_{b=1}^B q_b \widetilde{f}_b(z_N) \leq \sup_{\mathbf{f} \in \widetilde{\mathcal{F}}} \left[u(\mathbf{f}) - \sum_{b=1}^B f_b(z_N) \right] \quad (50)$$

Combine Eq. (48), Eq. (49) and Eq. (50):

$$\begin{aligned} (1 - \epsilon)A(\sigma_{N-1}) &\leq \frac{1}{2} \left[\sup_{\mathbf{f} \in \widehat{\mathcal{F}}} \left[u(\mathbf{f}) + \sum_{b=1}^B f_b(z_N) \right] + \sup_{\mathbf{f} \in \widetilde{\mathcal{F}}} \left[u(\mathbf{f}) - \sum_{b=1}^B f_b(z_N) \right] \right] \\ &= \mathbb{E}_{\sigma_N} \left\{ \sup_{\mathbf{f} \in \widehat{\mathcal{F}}} \left[u(\mathbf{f}) + \sigma_N \sum_{b=1}^B f_b(z_N) \right] \right\} \end{aligned} \quad (51)$$

Since Eq. (51) holds for every $\epsilon > 0$, we have that:

$$A(\sigma_{N-1}) \leq \mathbb{E}_{\sigma_N} \left\{ \sup_{\mathbf{f} \in \widehat{\mathcal{F}}} \left[u(\mathbf{f}) + \sigma_N \mathbf{1}^T \mathbf{f}(z_N) \right] \right\} \quad (52)$$

Repeating this process for the remaining σ s will eventually yield the result of this lemma. \square

APPENDIX E

PROOF OF THEOREM 3

Proof. Consider the function spaces:

$$\mathcal{G} \triangleq \{ \mathbf{g} : (x, l) \mapsto [\mu_1(l) f_1(x), \dots, \mu_B(l) f_B(x)]^T, \mu \in \mathcal{M}, \mathbf{f} : \mathcal{X} \mapsto \mathbb{R}^B \}$$

$$\Psi \circ \mathcal{G} \triangleq \left\{ \Psi(\mathbf{g}(\cdot)) : (x, l) \mapsto \frac{1}{B} \sum_{b=1}^B \Phi_\rho(g_b(x, l)), \mathbf{g} \in \mathcal{G} \right\}$$

Notice that, since $\Phi_\rho(u) \in [0, 1]$ for $\forall u \in \mathbb{R}$, also $\Psi(\mathbf{g}(x, l)) \in [0, 1]$ for $\forall \mathbf{g} \in \mathcal{G}, x \in \mathcal{X}$ and $l \in \mathbb{N}_G$. Hence, from Theorem 3.1 of [5], for fixed (independent of Q) $\rho > 0$ and for any $\delta > 0$ and any $\mathbf{g} \in \mathcal{G}$, with probability at least $1 - \delta$, it holds that:

$$\mathbb{E} \{ \Psi(\mathbf{g}(x, l)) \} \leq \widehat{\mathbb{E}}_Q \{ \Psi(\mathbf{g}(x, l)) \} + 2\mathfrak{R}_N(\Psi \circ \mathcal{G}) + \sqrt{\frac{\ln \frac{1}{\delta}}{2N}} \quad (53)$$

Where we define $\forall h : \mathcal{X} \times \mathbb{N}_G \mapsto \mathbb{R}$ and $\widehat{\mathbb{E}}_Q \{ h(x, l) \} \triangleq \frac{1}{N} \sum_{n=1}^N h(x_n, l_n)$. Since $[u < 0] \leq \Phi_\rho(u)$ for $\forall u \in \mathbb{R}, \rho > 0$, it holds that:

$$\begin{aligned} \frac{1}{B} d(\text{sgn } \mathbf{f}(x), \boldsymbol{\mu}(l)) &= \frac{1}{B} \sum_{b=1}^B [\mu_b(l) f_b(x) < 0] \leq \\ &\leq \frac{1}{B} \sum_{b=1}^B \Phi_\rho(\mu_b(l) f_b(x)) = \Psi(\mathbf{g}(x, l)) \end{aligned}$$

Thus, we have the following:

$$er(\mathbf{f}, \boldsymbol{\mu}) \triangleq \mathbb{E} \left\{ \frac{1}{B} d(\text{sgn } \mathbf{f}(x), \boldsymbol{\mu}(l)) \right\} \leq \mathbb{E} \{ \Psi(\mathbf{g}(x, l)) \} \quad (54)$$

Due to Eq. (54), with probability at least $1 - \delta$, Eq. (53) becomes now:

$$er(\mathbf{f}, \boldsymbol{\mu}) \leq \widehat{\mathbb{E}}_Q \{ \Psi(\mathbf{g}(x, l)) \} + 2\mathfrak{R}_N(\Psi \circ \mathcal{G}) + \sqrt{\frac{\ln \frac{1}{\delta}}{2N}} \quad (55)$$

Now due to the fact that $\Psi(\cdot)$ is $\frac{1}{B\rho}$ -Lipschitz continuous w.r.t $\|\cdot\|_1$ and Lemma 1, we have:

$$\widehat{\mathfrak{R}}_Q(\Psi \circ \mathcal{G}) \leq \frac{1}{B\rho} \widehat{\mathfrak{R}}_Q(\|\mathcal{G}\|_1)$$

Also, since $\boldsymbol{\mu} : \mathbb{N}_G \mapsto \mathbb{H}^B$, we have $\widehat{\mathfrak{R}}_Q(\|\mathcal{G}\|_1) = \widehat{\mathfrak{R}}_Q(\|\bar{\mathcal{F}}\|_1)$, where $\bar{\mathcal{F}}$ is defined in Eq. (18), we get:

$$\widehat{\mathfrak{R}}_Q(\Psi \circ \mathcal{G}) \leq \frac{1}{B\rho} \widehat{\mathfrak{R}}_Q(\|\bar{\mathcal{F}}\|_1)$$

Now due to Lemma 2, we have $\widehat{\mathfrak{R}}_Q(\|\bar{\mathcal{F}}\|_1) \leq \widehat{\mathfrak{R}}_Q(\mathbf{1}^T \bar{\mathcal{F}})$, by taking expectations on both sides w.r.t Q , the above inequality becomes:

$$\mathfrak{R}_N(\Psi \circ \mathcal{G}) \leq \frac{1}{B\rho} \mathfrak{R}_N(\mathbf{1}^T \bar{\mathcal{F}}) \quad (56)$$

Substitute Eq. (56) into Eq. (55):

$$er(\mathbf{f}, \boldsymbol{\mu}) \leq \widehat{\mathbb{E}}_Q \{ \Psi(\mathbf{g}(x, l)) \} + \frac{2}{B\rho} \mathfrak{R}_N(\mathbf{1}^T \bar{\mathcal{F}}) + \sqrt{\frac{\ln \frac{1}{\delta}}{2N}} \quad (57)$$

From the optimization problem in Eq. (6), we note that *SHL is utilizing the hypothesis spaces defined in Eq. (18) and Eq. (19). Note the fact that each hash function of *SHL is determined by the data independent of the others.

By considering the Representer Theorem [52], we have $w = \sum_{n=1} \alpha_n \Phi_{\theta}(x_n)$, $\boldsymbol{\alpha} \in \mathbb{R}^N$, which implies: $f(x) = \sum_n \alpha_n k_{\theta}(x, x_n) + \beta$ and $\|w\|_{\mathcal{H}_{\theta}}^2 = \boldsymbol{\alpha}^T \mathbf{K}_{\theta} \boldsymbol{\alpha}$. Here \mathbf{K}_{θ} is the kernel matrix of the training data.

Hence, \mathcal{F} can be re-expressed as:

$$\mathcal{F} = \left\{ f : x \mapsto \sum_n \alpha_n k_{\theta}(x, x_n) + \beta, \beta \in \mathbb{R}, \boldsymbol{\alpha} \in \Omega_{\alpha}(\boldsymbol{\theta}), \boldsymbol{\theta} \in \Omega_{\theta} \right\}$$

where $\Omega_{\alpha}(\boldsymbol{\theta}) \triangleq \{ \boldsymbol{\alpha} \in \mathbb{R}^N : \boldsymbol{\alpha}^T \mathbf{K}_{\theta} \boldsymbol{\alpha} \leq R^2 \}$.

First of all, let's upper bound the Rademacher Complexity of *SHL's hypothesis space:

$$\begin{aligned} \widehat{\mathfrak{R}}_Q(\mathbf{1}^T \bar{\mathcal{F}}) &= \frac{1}{N} \mathbb{E}_{\boldsymbol{\sigma}} \left\{ \sup_{\mathbf{f} \in \bar{\mathcal{F}}} \sum_n \sigma_n \sum_{b=1}^B f_b(x_n) \right\} = \\ &= \frac{1}{N} \mathbb{E}_{\boldsymbol{\sigma}} \left\{ \sup_{f_b \in \mathcal{F}, b \in \mathbb{N}_B} \sum_b \sum_n \sigma_n f_b(x_n) \right\} = \\ &= \sum_b \frac{1}{N} \mathbb{E}_{\boldsymbol{\sigma}} \left\{ \sup_{f_b \in \mathcal{F}} \sum_n \sigma_n f_b(x_n) \right\} = B \widehat{\mathfrak{R}}_Q(\mathcal{F}) \quad (58) \end{aligned}$$

Next, we will upper bound $\widehat{\mathfrak{R}}_Q(\mathcal{F})$:

$$\begin{aligned} \widehat{\mathfrak{R}}_Q(\mathcal{F}) &= \frac{1}{N} \mathbb{E}_{\boldsymbol{\sigma}} \left\{ \sup_{f \in \mathcal{F}} \sum_n \sigma_n f(x_n) \right\} = \\ &= \mathbb{E}_{\boldsymbol{\sigma}} \left\{ \sup_{\boldsymbol{\alpha} \in \Omega_{\alpha}(\boldsymbol{\theta}), \boldsymbol{\theta} \in \Omega_{\theta}} \boldsymbol{\alpha}^T \mathbf{K}_{\theta} \boldsymbol{\alpha} + \sup_{\beta \in \mathbb{R}} \sum_n \sigma_n \beta \right\} \leq \\ &\leq \frac{R}{N} \mathbb{E}_{\boldsymbol{\sigma}} \left\{ \sup_{\boldsymbol{\theta} \in \Omega_{\theta}} \sqrt{\boldsymbol{\alpha}^T \mathbf{K}_{\theta} \boldsymbol{\alpha}} \right\} = \frac{R}{N} \mathbb{E}_{\boldsymbol{\sigma}} \left\{ \sqrt{\sup_{\boldsymbol{\theta} \in \Omega_{\theta}} \boldsymbol{\theta}^T \mathbf{u}} \right\} \quad (59) \end{aligned}$$

where $\mathbf{u} \in \mathbb{R}^M$ such that $u_m \triangleq \boldsymbol{\sigma}^T \mathbf{K}_m \boldsymbol{\alpha}$. The above inequality holds because of Cauchy-Schwarz inequality. Additionally, $\mathbb{E}_{\boldsymbol{\sigma}} \{ \sup_{\beta \in \mathbb{R}} \sum_n \sigma_n \beta \} = 0$ since β is bounded.

By the definition of the dual norm, if $p' \triangleq \frac{p}{p-1}$, we have:

$$\sup_{\boldsymbol{\theta} \in \Omega_{\theta}} \boldsymbol{\theta}^T \mathbf{u} = \|\mathbf{u}\|_{p'} \quad (60)$$

Thus, Eq. (59) becomes:

$$\begin{aligned} \widehat{\mathfrak{R}}_Q(\mathcal{F}) &\leq \frac{R}{N} \mathbb{E}_{\boldsymbol{\sigma}} \left\{ \sqrt{\|\mathbf{u}\|_{p'}} \right\} = \\ &= \frac{R}{N} \mathbb{E}_{\boldsymbol{\sigma}} \left\{ \left[\sum_{m=1}^M (\boldsymbol{\sigma}^T \mathbf{K}_m \boldsymbol{\sigma})^{p'} \right]^{\frac{1}{2p'}} \right\} \leq \\ &\leq \frac{R}{N} \left[\sum_m \mathbb{E}_{\boldsymbol{\sigma}} \left\{ (\boldsymbol{\sigma}^T \mathbf{K}_m \boldsymbol{\sigma})^{p'} \right\} \right]^{\frac{1}{2p'}} \end{aligned}$$

The above inequality holds because of Jensen's Inequality. By the Lemma 5 from [53], the above expression is upper bounded by:

$$\begin{aligned} &\frac{R}{N} \left[\sum_m (p')^{\frac{p'}{2}} (\text{trace} \{ \mathbf{K}_m \})^{\frac{p'}{2}} \right]^{\frac{1}{2p'}} = \\ &= \frac{R}{N} (p')^{\frac{1}{4}} \left[\sum_m [\text{trace} \{ \mathbf{K}_m \}]^{\frac{p'}{2}} \right]^{\frac{1}{2p'}} \quad (61) \end{aligned}$$

Since $k_m(x, x') \leq r^2$, $\forall m \in \mathbb{N}_M$, $x \in \mathcal{X}$:

$$\begin{aligned} \text{trace} \{ \mathbf{K}_m \} &\leq N r^2 \Rightarrow [\text{trace} \{ \mathbf{K}_m \}]^{\frac{p'}{2}} \leq N^{\frac{p'}{2}} r^{p'} \Rightarrow \\ &\Rightarrow \left[\sum_m [\text{trace} \{ \mathbf{K}_m \}]^{\frac{p'}{2}} \right]^{\frac{1}{2p'}} \leq M^{\frac{1}{p'}} N^{\frac{1}{4}} r^{\frac{1}{2}} \quad (62) \end{aligned}$$

Thus, combine Eq. (61) and Eq. (62), we have:

$$\widehat{\mathfrak{R}}_Q(\mathcal{F}) \leq \frac{R}{N} q^{\frac{1}{4}} M^{\frac{1}{2p'}} N^{\frac{1}{4}} r^{\frac{1}{2}} = R \left(\frac{p'}{N^3} \right)^{\frac{1}{4}} \sqrt{r M^{\frac{1}{p'}}} \quad (63)$$

Combine Eq. (58) and Eq. (63):

$$\begin{aligned} \widehat{\mathfrak{R}}_Q(\mathbf{1}^T \bar{\mathcal{F}}) &\leq B R \left(\frac{p'}{N^3} \right)^{\frac{1}{4}} \sqrt{r M^{\frac{1}{p'}}} \Rightarrow \\ &\Rightarrow \mathfrak{R}_N(\mathbf{1}^T \bar{\mathcal{F}}) \leq B R \sqrt{r M^{\frac{1}{p'}}} \sqrt{\frac{p'}{N^3}} \quad (64) \end{aligned}$$

Finally, combine Eq. (57) and Eq. (64), one can generate the bound provided in Theorem 3. \square

ACKNOWLEDGMENTS

Y. Huang acknowledges partial support from a UCF Graduate College Presidential Fellowship and National Science Foundation(NSF) grant No. 1200566. Furthermore, M. Georgiopoulos acknowledges partial support from NSF grants No. 1161228 and No. 0525429, while G. C. Anagnostopoulos acknowledges partial support from NSF grant No. 1263011. Note that any opinions, findings, and conclusions or recommendations expressed in this material are those of the authors and do not necessarily reflect the views of the NSF. Finally, the authors would like to thank the reviewers of this manuscript for their helpful comments.

REFERENCES

- [1] R. Datta, D. Joshi, J. Li, and J. Z. Wang, "Image retrieval: Ideas, influences, and trends of the new age," *ACM Computing Surveys*, vol. 40, no. 2, pp. 5:1–5:60, May 2008.
- [2] A. Torralba, R. Fergus, and Y. Weiss, "Small codes and large image databases for recognition," in *Proceedings of Computer Vision and Pattern Recognition*, 2008, pp. 1–8.
- [3] Y. Huang, M. Georgiopoulos, and G. C. Anagnostopoulos, "Hash function learning via codewords," in *Machine Learning and Knowledge Discovery in Databases*, 2015, pp. 659–674.
- [4] T. G. Dietterich and G. Bakiri, "Solving multiclass learning problems via error-correcting output codes," *Journal of Artificial Intelligence Research*, vol. 2, no. 1, pp. 263–286, Jan. 1995.
- [5] M. Mohri, A. Rostamizadeh, and A. Talwalkar, *Foundations of Machine Learning*. The MIT Press, 2012.
- [6] M. Kloft, U. Brefeld, S. Sonnenburg, and A. Zien, "lp-norm multiple kernel learning," *Journal of Machine Learning Research*, vol. 12, pp. 953–997, Jul. 2011.
- [7] C.-C. Chang and C.-J. Lin, "LIBSVM: A library for support vector machines," *ACM Transactions on Intelligent Systems and Technology*, vol. 2, pp. 27:1–27:27, 2011, software available at <http://www.csie.ntu.edu.tw/~cjlin/libsvm>.
- [8] V. Sindhwani and H. Avron, "High-performance kernel machines with implicit distributed optimization and randomization," *arXiv preprint arXiv:1409.0940*, 2014.
- [9] A. Gionis, P. Indyk, and R. Motwani, "Similarity search in high dimensions via hashing," in *Proceedings of the International Conference on Very Large Data Bases*, 1999, pp. 518–529.
- [10] B. Kulis, P. Jain, and K. Grauman, "Fast similarity search for learned metrics," *IEEE Transactions on Pattern Analysis and Machine Intelligence*, vol. 31, no. 12, pp. 2143–2157, 2009.
- [11] M. Raginsky and S. Lazebnik, "Locality-sensitive binary codes from shift-invariant kernels," in *Proceedings of Advanced Neural Information Processing Systems*, 2009, pp. 1509–1517.
- [12] R. Salakhutdinov and G. Hinton, "Semantic hashing," *International Journal of Approximate Reasoning*, vol. 50, no. 7, pp. 969–978, Jul. 2009.
- [13] B. Kulis and T. Darrell, "Learning to hash with binary reconstructive embeddings," in *Proceedings of Advanced Neural Information Processing Systems*, 2009, pp. 1042–1050.
- [14] M. Norouzi and D. J. Fleet, "Minimal loss hashing for compact binary codes," in *Proceedings of the International Conference on Machine Learning*, 2011, pp. 353–360.
- [15] C.-N. J. Yu and T. Joachims, "Learning structural svms with latent variables," in *Proceedings of the International Conference on Machine Learning*, 2009, pp. 1169–1176.
- [16] Y. Mu, J. Shen, and S. Yan, "Weakly-supervised hashing in kernel space," in *Proceedings of Computer Vision and Pattern Recognition*, 2010, pp. 3344–3351.
- [17] D. Zhang, J. Wang, D. Cai, and J. Lu, "Self-taught hashing for fast similarity search," in *Proceedings of the International Conference on Research and Development in Information Retrieval*, 2010, pp. 18–25.
- [18] C. Strecha, A. Bronstein, M. Bronstein, and P. Fua, "Ldashash: Improved matching with smaller descriptors," *IEEE Transactions on Pattern Analysis and Machine Intelligence*, vol. 34, no. 1, pp. 66–78, 2012.
- [19] G. Shakhnarovich, P. Viola, and T. Darrell, "Fast pose estimation with parameter-sensitive hashing," in *Proceedings of the International Conference on Computer Vision*, 2003, pp. 750–.
- [20] S. Baluja and M. Covell, "Learning to hash: Forgiving hash functions and applications," *Data Mining and Knowledge Discovery*, vol. 17, no. 3, pp. 402–430, 2008.
- [21] X. Li, G. Lin, C. Shen, A. van den Hengel, and A. R. Dick, "Learning hash functions using column generation," in *Proceedings of the International Conference on Machine Learning*, 2013, pp. 142–150.
- [22] W. Liu, J. Wang, R. Ji, Y.-G. Jiang, and S.-F. Chang, "Supervised hashing with kernels," in *Proceedings of Computer Vision and Pattern Recognition*, 2012, pp. 2074–2081.
- [23] G. Lin, C. Shen, Q. Shi, A. van den Hengel, and D. Suter, "Fast supervised hashing with decision trees for high-dimensional data," in *Proceedings of Computer Vision and Pattern Recognition*, 2014.
- [24] R. Xia, Y. Pan, H. Lai, and S. Yan, "Supervised hashing for image retrieval via image representation learning," in *Proceedings of the AAAI Conference on Artificial Intelligence*, 2014.
- [25] P. Zhang, W. Zhang, W.-J. Li, and M. Guo, "Supervised hashing with latent factor models," in *Proceedings of the International Conference on Research and Development in Information Retrieval*, 2014, pp. 173–182.
- [26] G. Lin, C. Shen, and J. Wu, "Optimizing ranking measures for compact binary code learning," in *Proceedings of European Conference on Computer Vision*, vol. 8691, 2014, pp. 613–627.
- [27] Y. Weiss, A. Torralba, and R. Fergus, "Spectral hashing," in *Proceedings of Advanced Neural Information Processing Systems*, 2008, pp. 1753–1760.
- [28] L. Chen, D. Xu, I.-H. Tsang, and X. Li, "Spectral embedded hashing for scalable image retrieval," *IEEE Transactions on Cybernetics*, vol. 44, no. 7, pp. 1180–1190, July 2014.
- [29] W. Liu, J. Wang, S. Kumar, and S.-F. Chang, "Hashing with graphs," in *Proceedings of the International Conference on Machine Learning*, 2011, pp. 1–8.
- [30] J. Wang, S. Kumar, and S.-F. Chang, "Sequential projection learning for hashing with compact codes," in *Proceedings of the International Conference on Machine Learning*, 2010, pp. 1127–1134.
- [31] Y. Gong and S. Lazebnik, "Iterative quantization: A procrustean approach to learning binary codes," in *Proceedings of Computer Vision and Pattern Recognition*, 2011, pp. 817–824.
- [32] X. Liu, Y. Mu, D. Zhang, B. Lang, and X. Li, "Large-scale unsupervised hashing with shared structure learning," *IEEE Transactions on Cybernetics*, vol. PP, no. 99, pp. 1–1, 2014.
- [33] W. Liu, C. Mu, S. Kumar, and S. fu Chang, "Discrete graph hashing," in *Proceedings of Advances in Neural Information Processing Systems*, 2014, pp. 3419–3427.
- [34] J. Wang, S. Kumar, and S.-F. Chang, "Semi-supervised hashing for large-scale search," *IEEE Transactions on Pattern Analysis and Machine Intelligence*, vol. 34, no. 12, pp. 2393–2406, 2012.
- [35] Q. Wang, L. Si, and D. Zhang, "Learning to hash with partial tags: Exploring correlation between tags and hashing bits for large scale image retrieval," in *Proceedings of European Conference on Computer Vision*, vol. 8691, 2014, pp. 378–392.
- [36] J. Cheng, C. Leng, P. Li, M. Wang, and H. Lu, "Semi-supervised multi-graph hashing for scalable similarity search," *Computer Vision and Image Understanding*, vol. 124, pp. 12 – 21, 2014.
- [37] D. R. Hunter and K. Lange, "A tutorial on mm algorithms," *The American Statistician*, vol. 58, no. 1, pp. 30–37, 2004.
- [38] —, "Quantile regression via an mm algorithm," *Journal of Computational and Graphical Statistics*, vol. 9, no. 1, pp. 60–77, Mar 2000.
- [39] A. Rahimi and B. Recht, "Random features for large-scale kernel machines," in *Proceedings of Advanced Neural Information Processing Systems*, 2008, pp. 1177–1184.
- [40] N. Parikh and S. Boyd, "Block splitting for distributed optimization," *Mathematical Programming Computation*, vol. 6, no. 1, pp. 77–102, 2014.
- [41] —, "Proximal algorithms," *Foundations and Trends in Optimization*, vol. 1, no. 3, 2014.
- [42] Y. Huang, C. Li, M. Georgiopoulos, and G. Anagnostopoulos, "Reduced-rank local distance metric learning," in *Machine Learning and Knowledge Discovery in Databases*, vol. 8190, 2013, pp. 224–239.

- [43] X. Chen, W. Pan, J. T. Kwok, and J. G. Carbonell, "Accelerated gradient method for multi-task sparse learning problem." in *Proceedings of the International Conference on Data Mining*, 2009, pp. 746–751.
- [44] A. Rakotomamonjy, R. Flamary, G. Gasso, and S. Canu, "lp-lq penalty for sparse linear and sparse multiple kernel multi-task learning," *IEEE Transactions on Neural Networks*, vol. 22, no. 8, pp. 1307–1320, 2011.
- [45] Y.-L. Yu, "Better approximation and faster algorithm using the proximal average," in *Proceedings of Advances in Neural Information Processing Systems 26*, 2013, pp. 458–466.
- [46] A. Beck and M. Teboulle, "Gradient-based algorithms with applications to signal recovery," *Convex Optimization in Signal Processing and Communications*, pp. 42–88, 2009.
- [47] N. List and H. U. Simon, "Svm-optimization and steepest-descent line search," in *Proceedings of the Conference on Computational Learning Theory*, 2009.
- [48] M. Everingham, L. Gool, C. K. Williams, J. Winn, and A. Zisserman, "The pascal visual object classes (voc) challenge," *International Journal of Computer Vision*, vol. 88, no. 2, pp. 303–338, Jun. 2010.
- [49] V. N. Vapnik, *Statistical Learning Theory*. Wiley-Interscience, 1998.
- [50] A. Blake, C. Rother, M. Brown, P. Perez, and P. Torr, "Interactive image segmentation using an adaptive gmmrf model," in *Proceedings of the European Conference in Computer Vision*, May 2004.
- [51] V. Gulshan, C. Rother, A. Criminisi, A. Blake, and A. Zisserman, "Geodesic star convexity for interactive image segmentation," in *Proceedings of the Conference on Computer Vision and Pattern Recognition*, 2010.
- [52] B. Schölkopf, R. Herbrich, and A. J. Smola, "A generalized representer theorem," in *Proceedings of the European Conference on Computational Learning Theory*, 2001, pp. 416–426.
- [53] C. Li, M. Georgiopoulos, and G. C. Anagnostopoulos, "Multi-task classification hypothesis space with improved generalization bounds," *Neural Networks and Learning Systems, IEEE Transactions on*, vol. 26, pp. 1468–1479, 2015.